

# **Badanie mechanizmów plastyczności w steksturyowanym stopie magnezu AZ31 przy użyciu dyfrakcji neutronowej**

***Plastic deformation study in textured AZ31 magnesium alloy using neutron diffraction***

P. Kot<sup>1</sup>, A. Baczmański<sup>2</sup>, A. Ludwik<sup>2</sup>, M. Wroński<sup>2</sup>, J. Pilch<sup>3</sup>, G. Farkas<sup>3</sup>, S. Wroński<sup>2</sup>

<sup>1</sup>CoE NOMATEN, National Institute for Nuclear Research, A. Sołtana 7, 05-400 Otwock, Poland

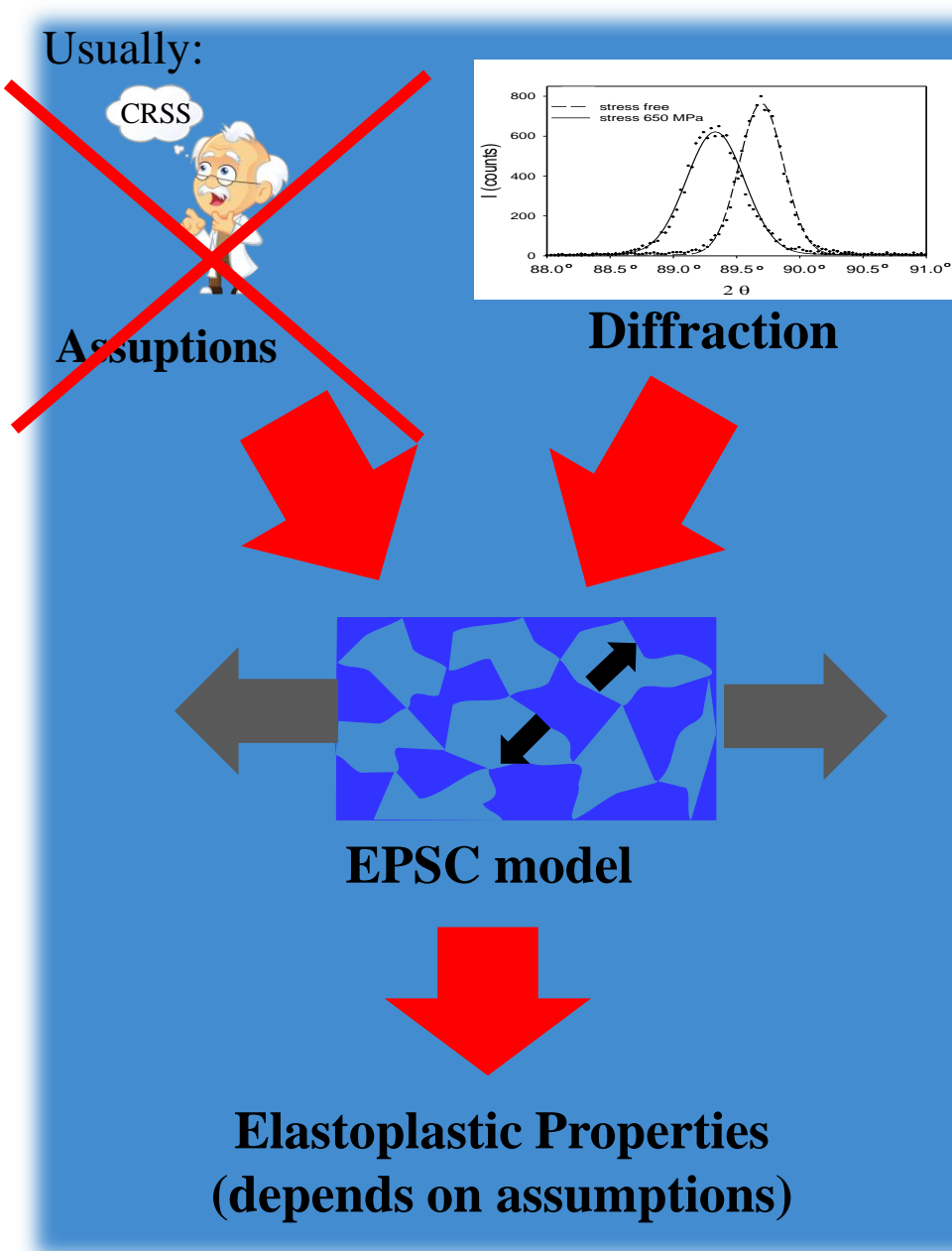
<sup>2</sup>AGH University of Science and Technology, WFiS, al. Mickiewicza 30, 30-059 Kraków, Poland

<sup>3</sup>Nuclear Physical Institute, ASCR, Hlavni 130, 25068 Řež, Czech Republic

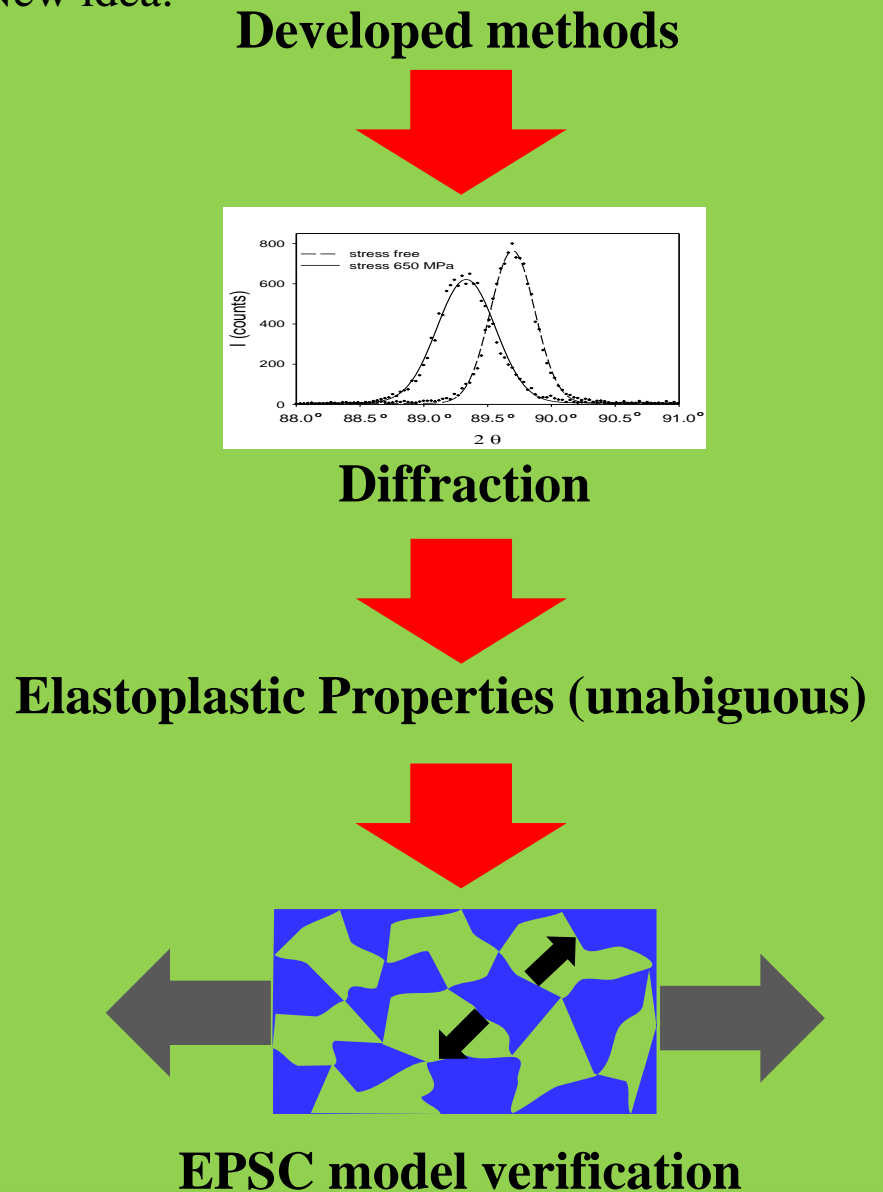
# **Agenda**

- 1. Aim of the study**
- 2. Material characterisation**
- 3. Crystallite group method**
- 4. Stress localisation**
- 5. Direct measurement of CRSS**
- 6. Cycling load & detwinning**

# Aims of the study



New idea:

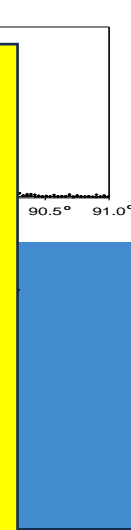


# Aims of the study

Usually:

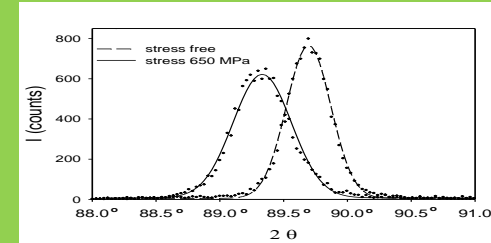
How to get  
Elastic properties  
**directly from**  
experiment?

(depends on assumptions)



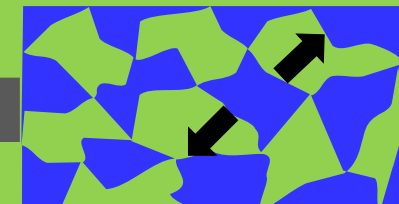
New idea:

Developed methods



Diffraction

Elastoplastic Properties (unambiguous)

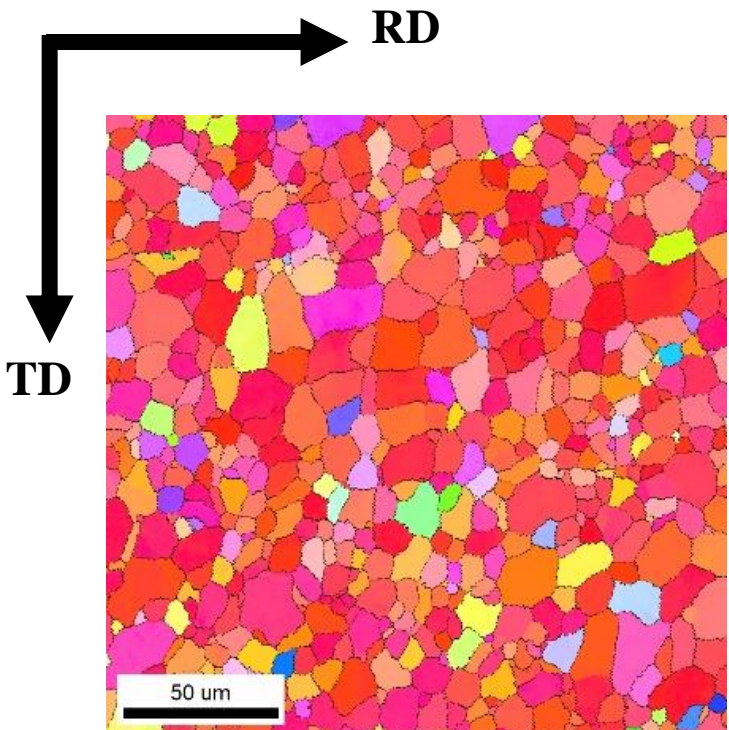


EPSC model verification

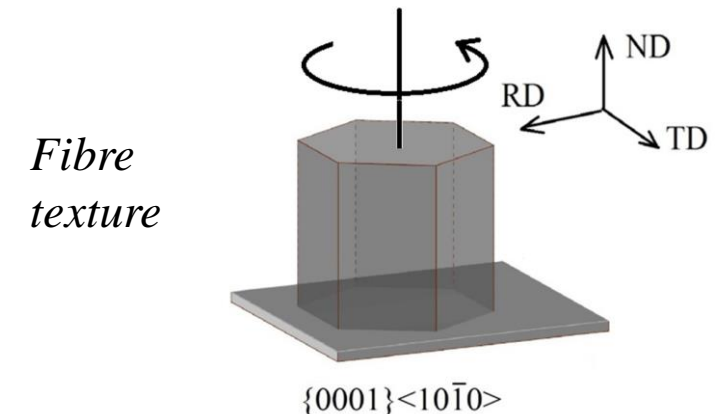
# Grain stresses – textured Mg alloy

# Material characterization Mg alloy (AZ31) – hot rolled

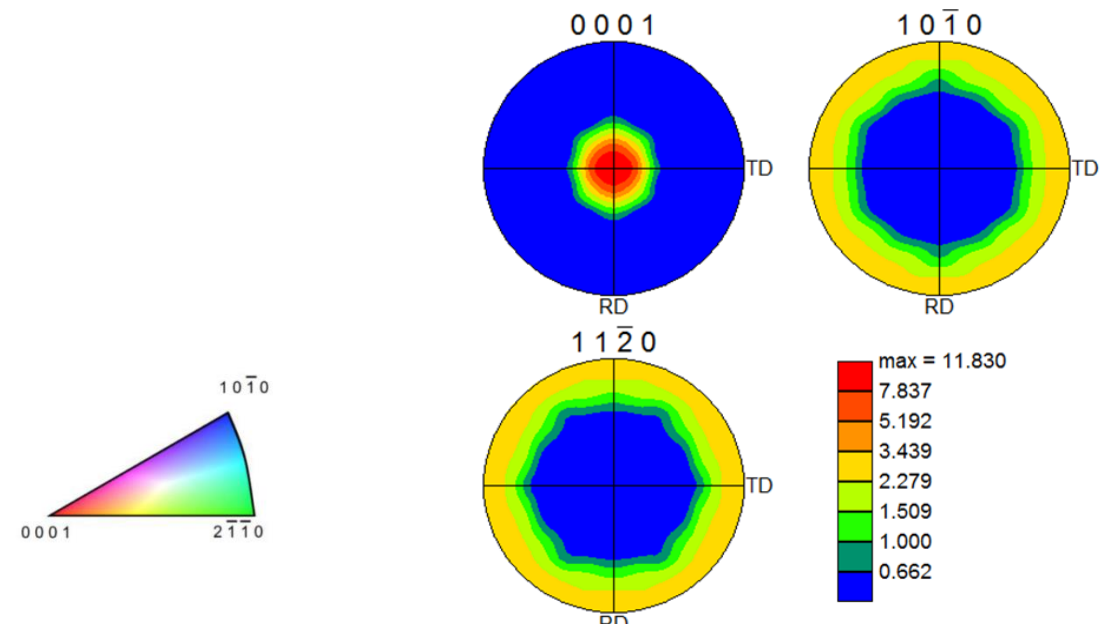
	Al	Zn	Mn	Cu	Mg
wt%	2,5-3,5	0,7-1,3	0,2-1,0	0,05	94,15-96,55



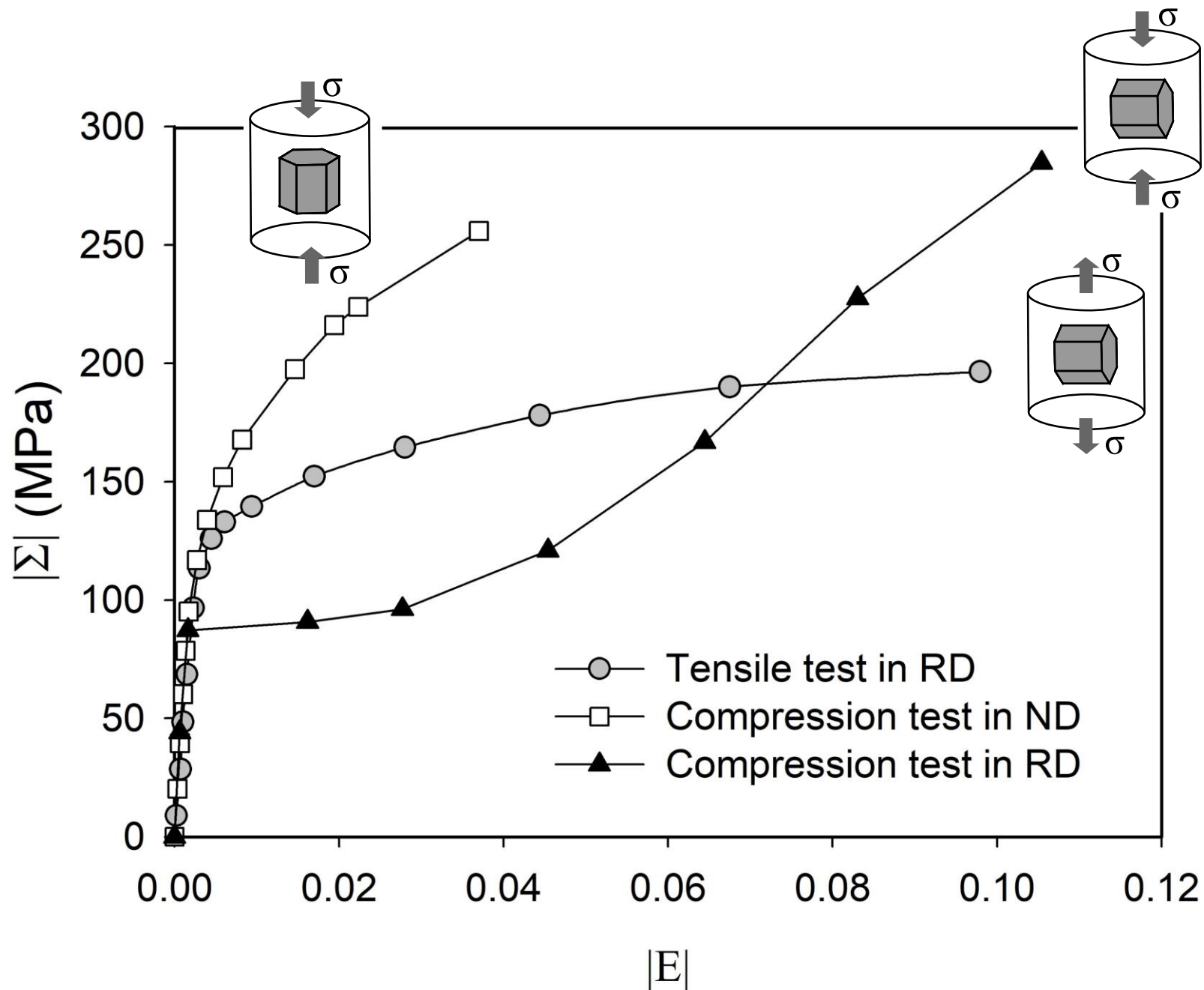
Orientation map from EBSD



Crystallographic texture



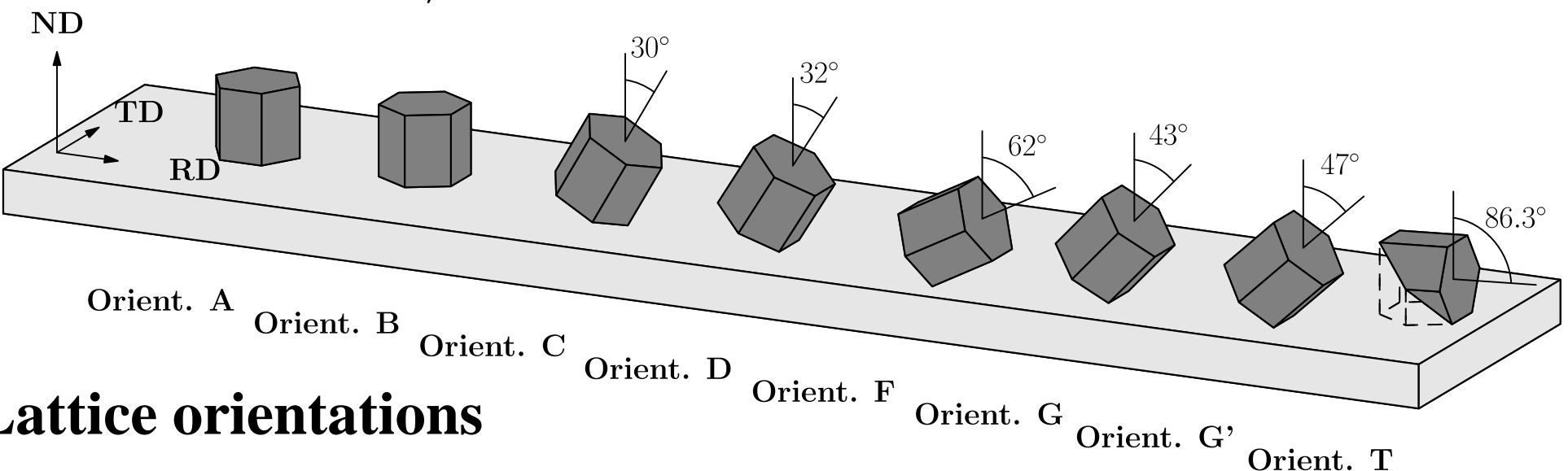
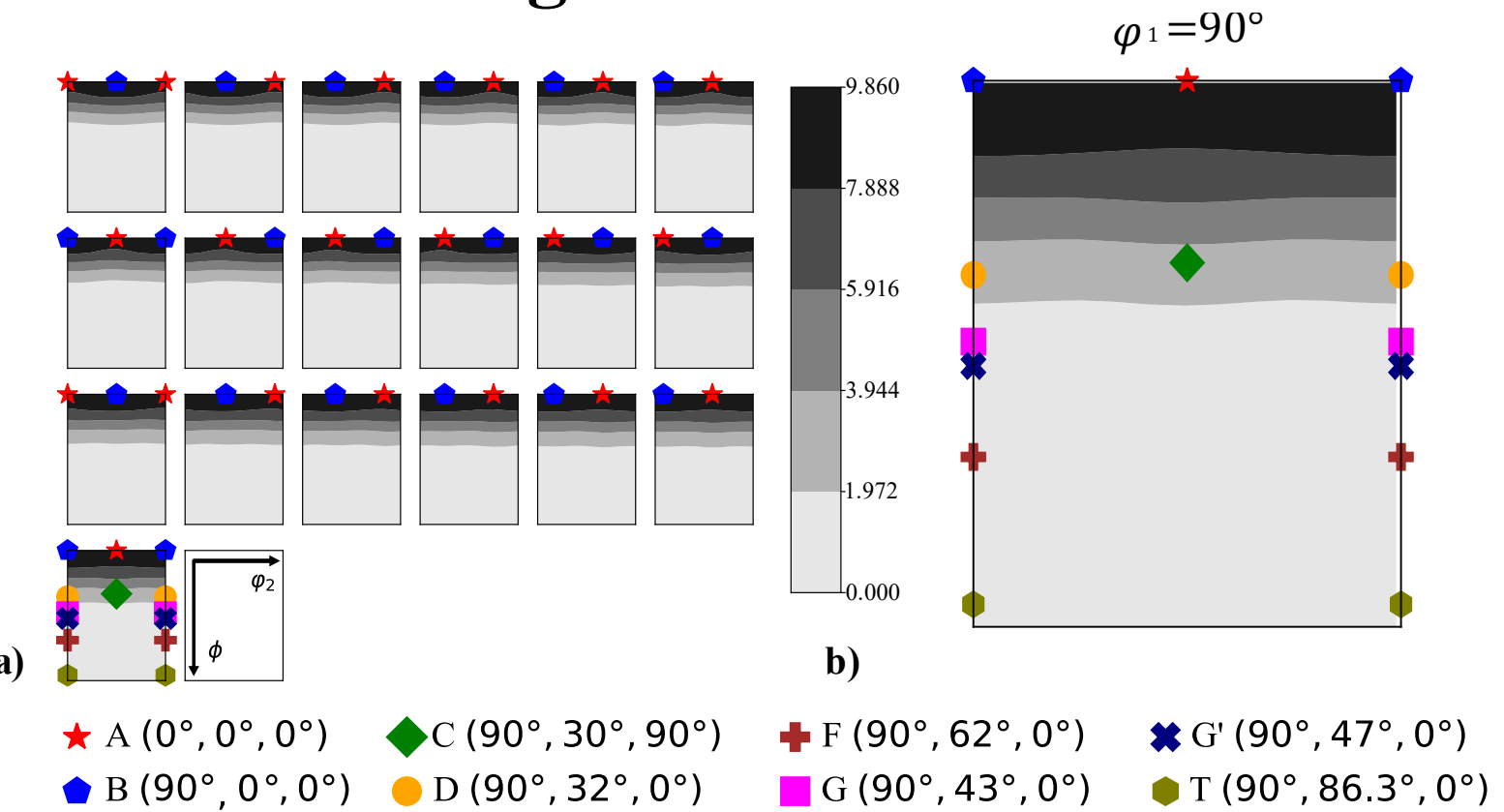
# Mg alloy (AZ31) – anisotropy



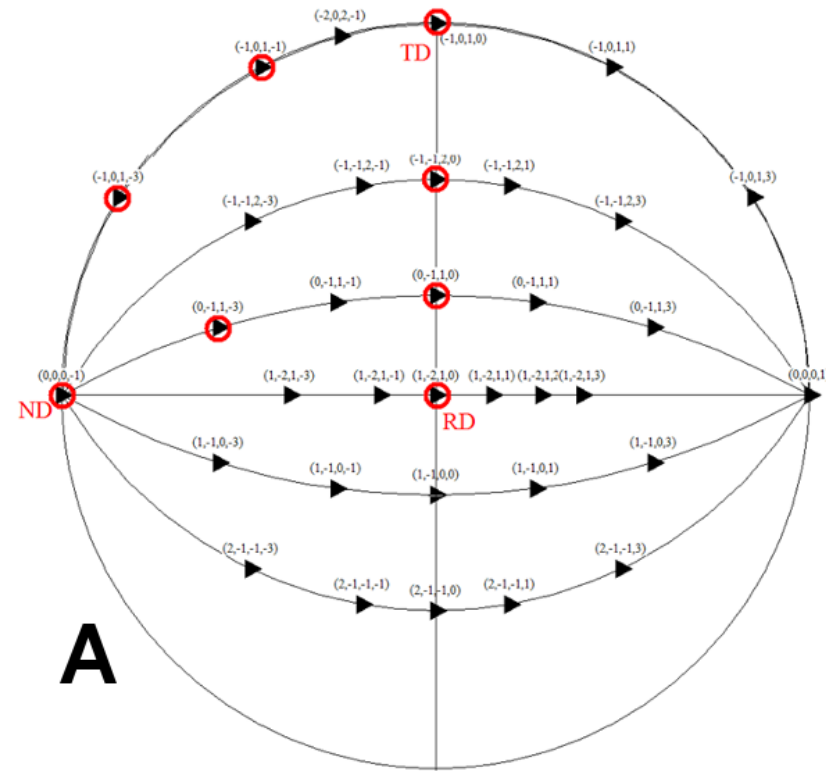
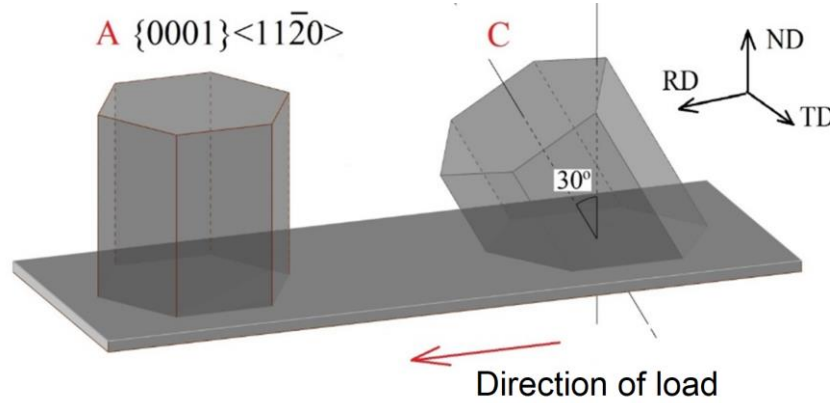
# Crystallite Group Method

# Chosen grain orientations

**Orientation  
Distribution  
Function**

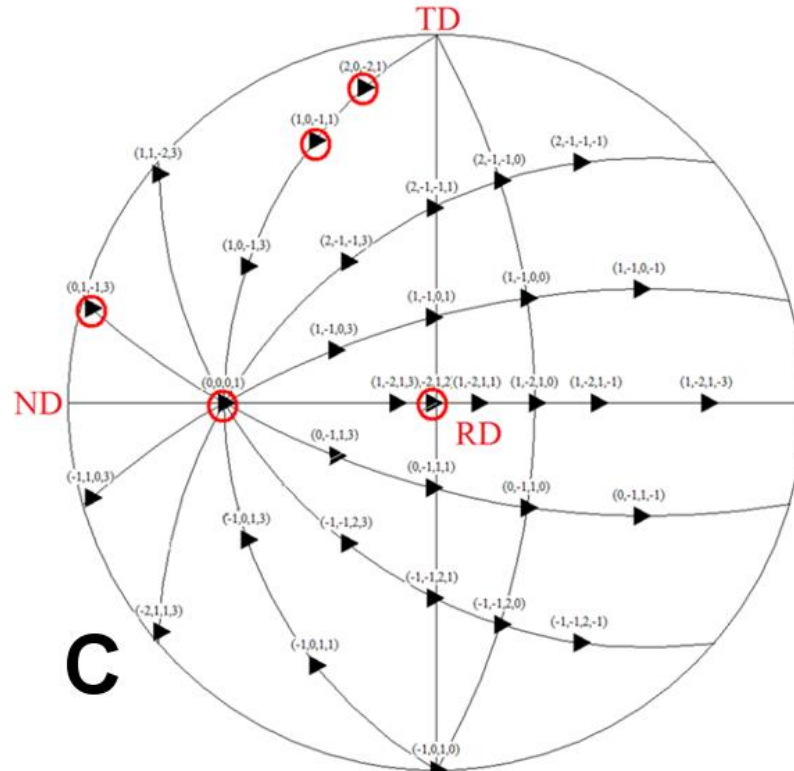


# Crystallite group method



**Least squares fitting**

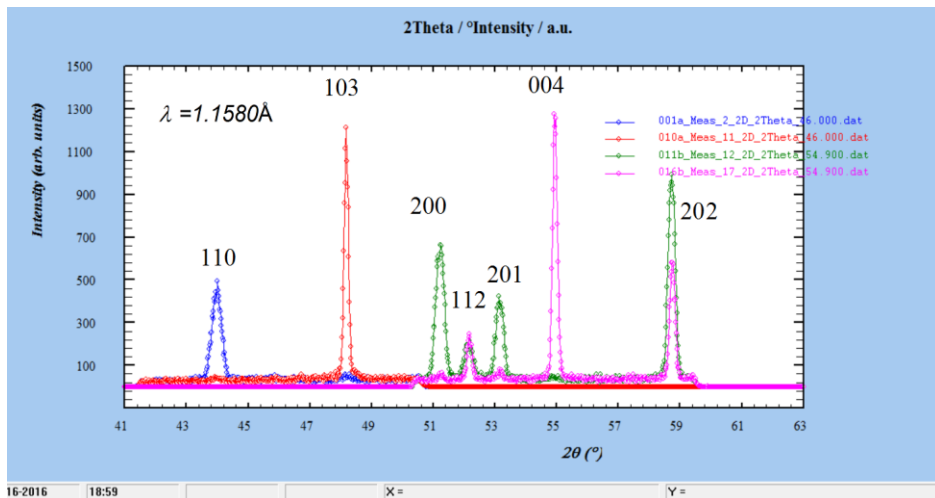
$$\langle \varepsilon(\psi, \varphi) \rangle_{\{hkl\}} = \langle \gamma_{3i} \gamma_{3j} s_{33ij}^g \rangle_{\{hkl\}} \sigma_{ij}^g$$



# Monotonic load experiments for Mg alloy

# Experiment at HK9, NPI, Řež/Prague tensile in RD (RDT)

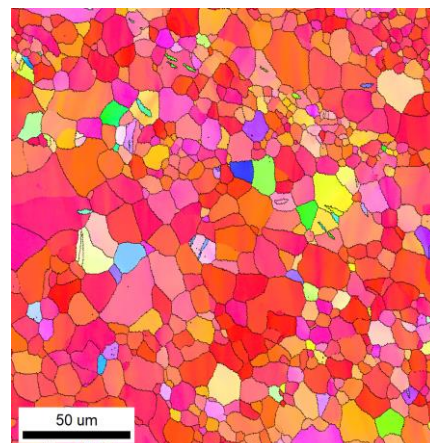
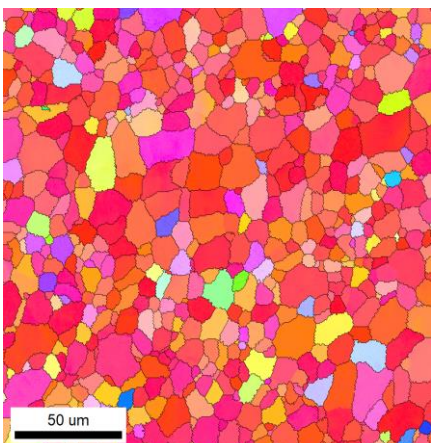
Monochromatic wavelength:  $\lambda=1.158 \text{ \AA}$



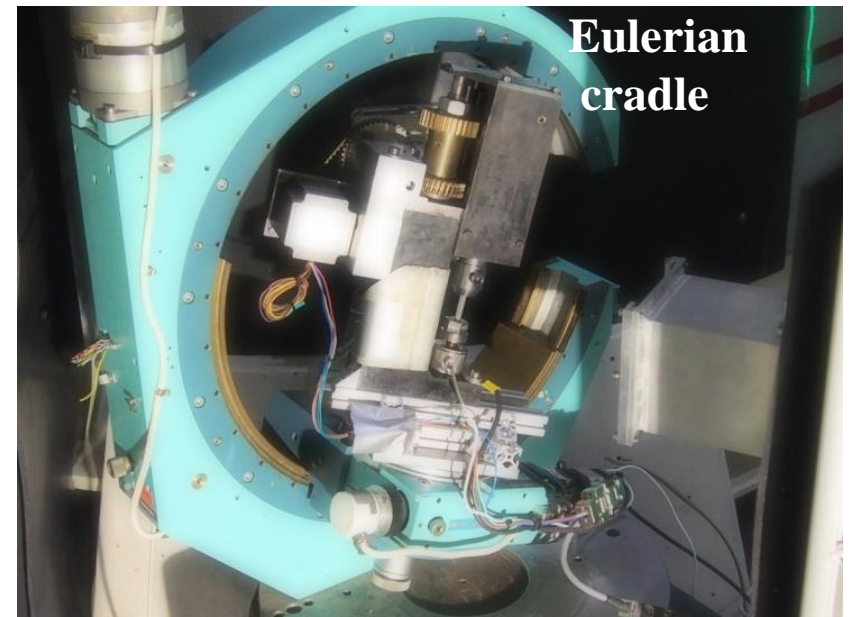
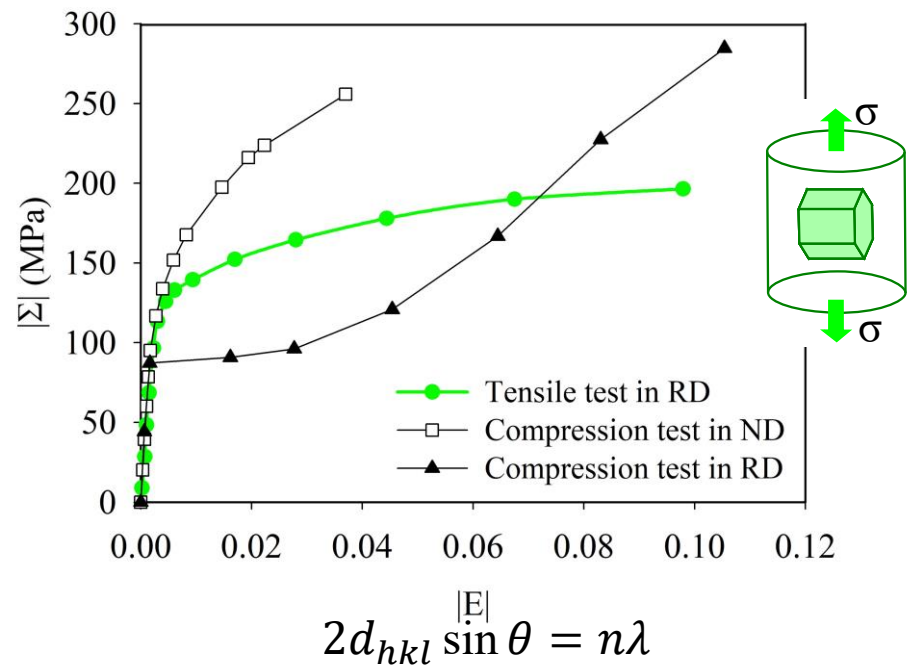
$$2d_{hkl} \sin \theta = n\lambda$$

RDT

Initial state



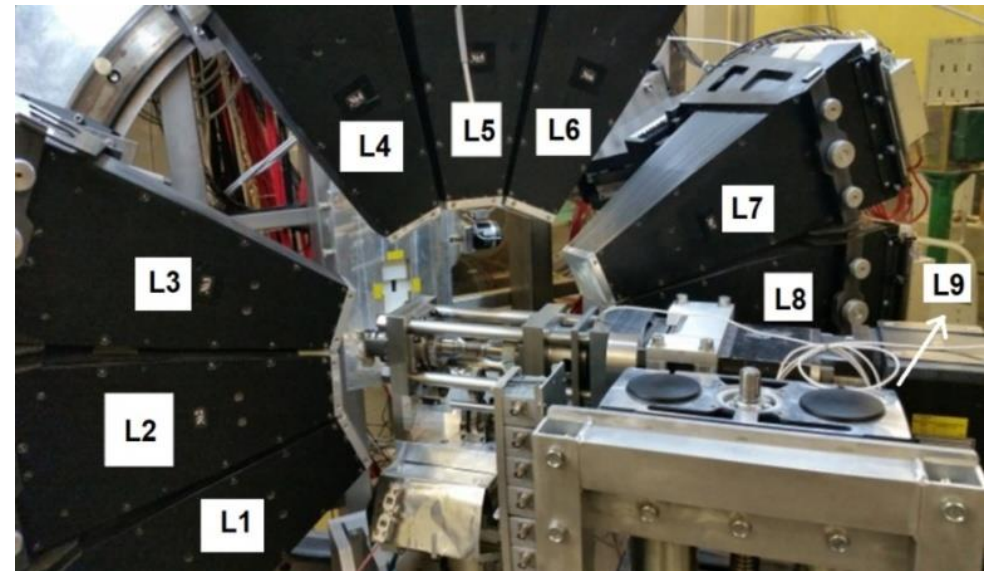
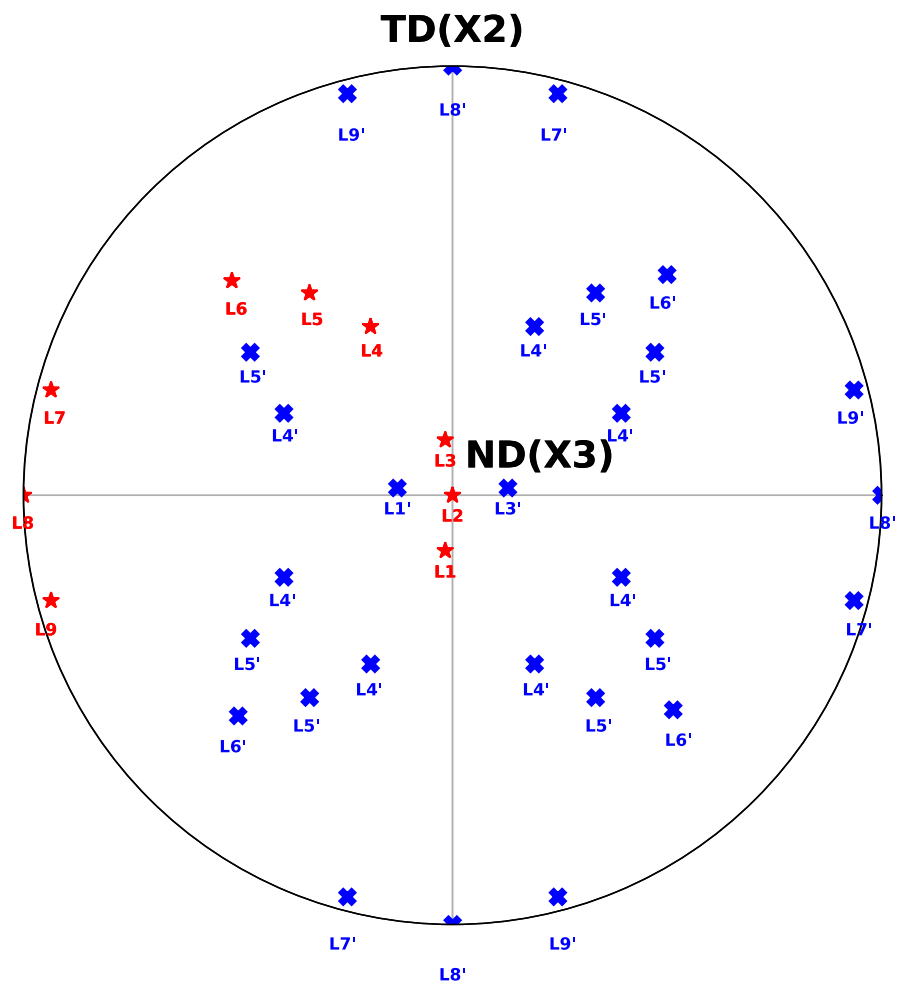
$$\varepsilon = 2\%$$



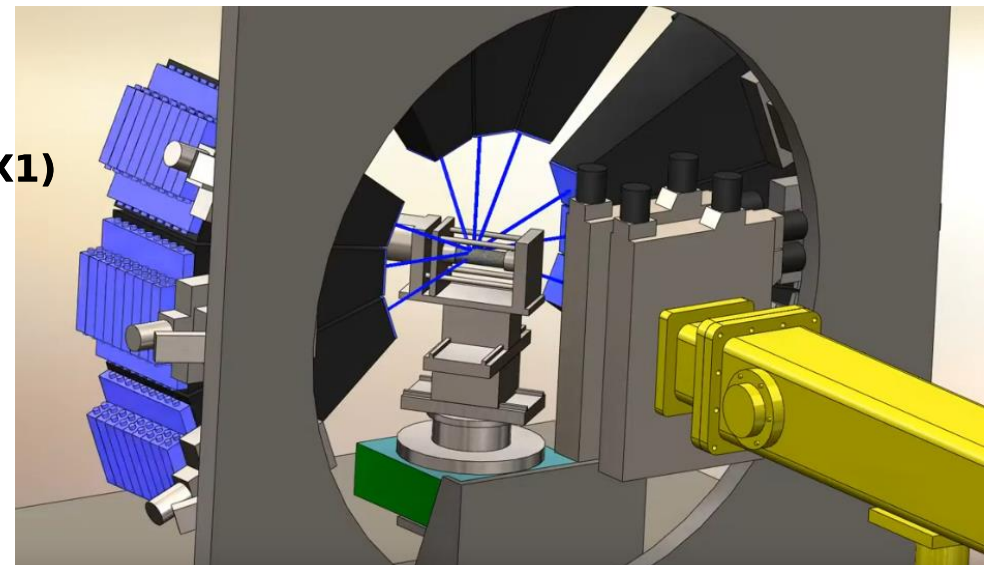
# TOF diffraction in JINR Dubna, Russia (**NDC** and **RDC**)

**Time of Flight:**  $d_{hkl} = \frac{hT}{2mL\sin \theta}$

$$2\theta = 90^\circ$$



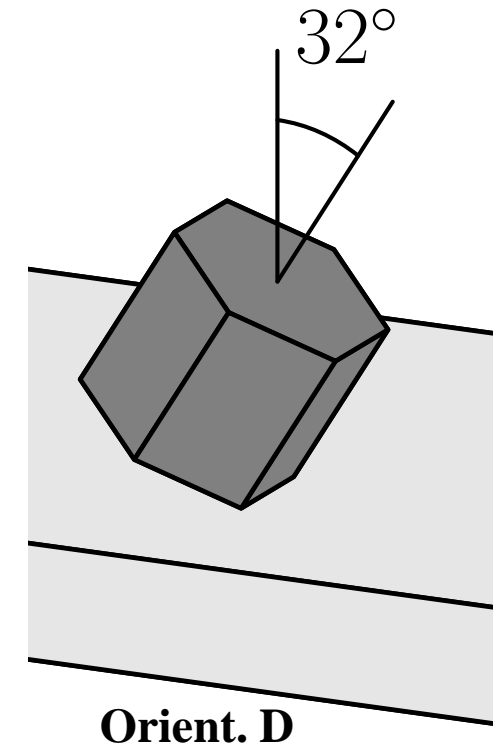
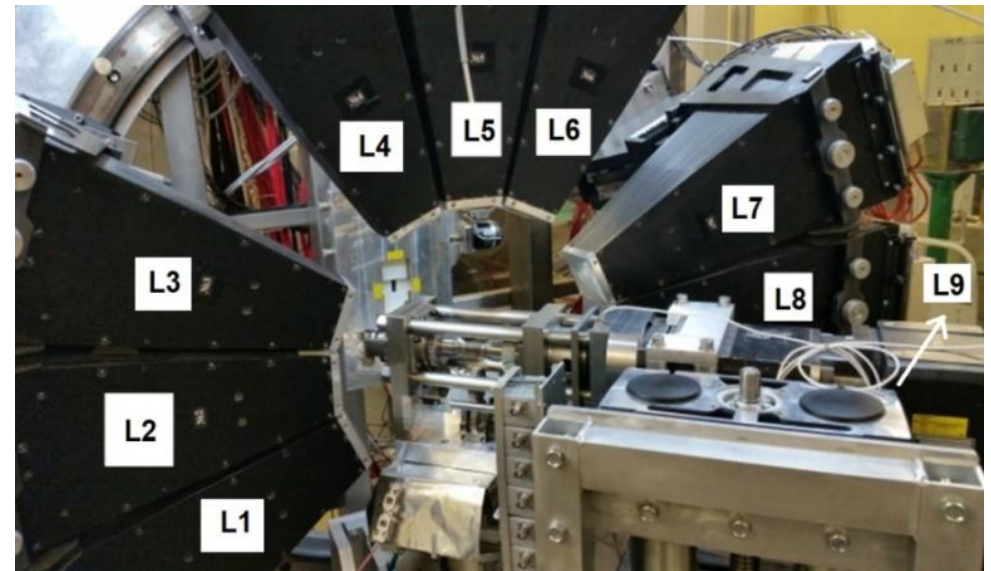
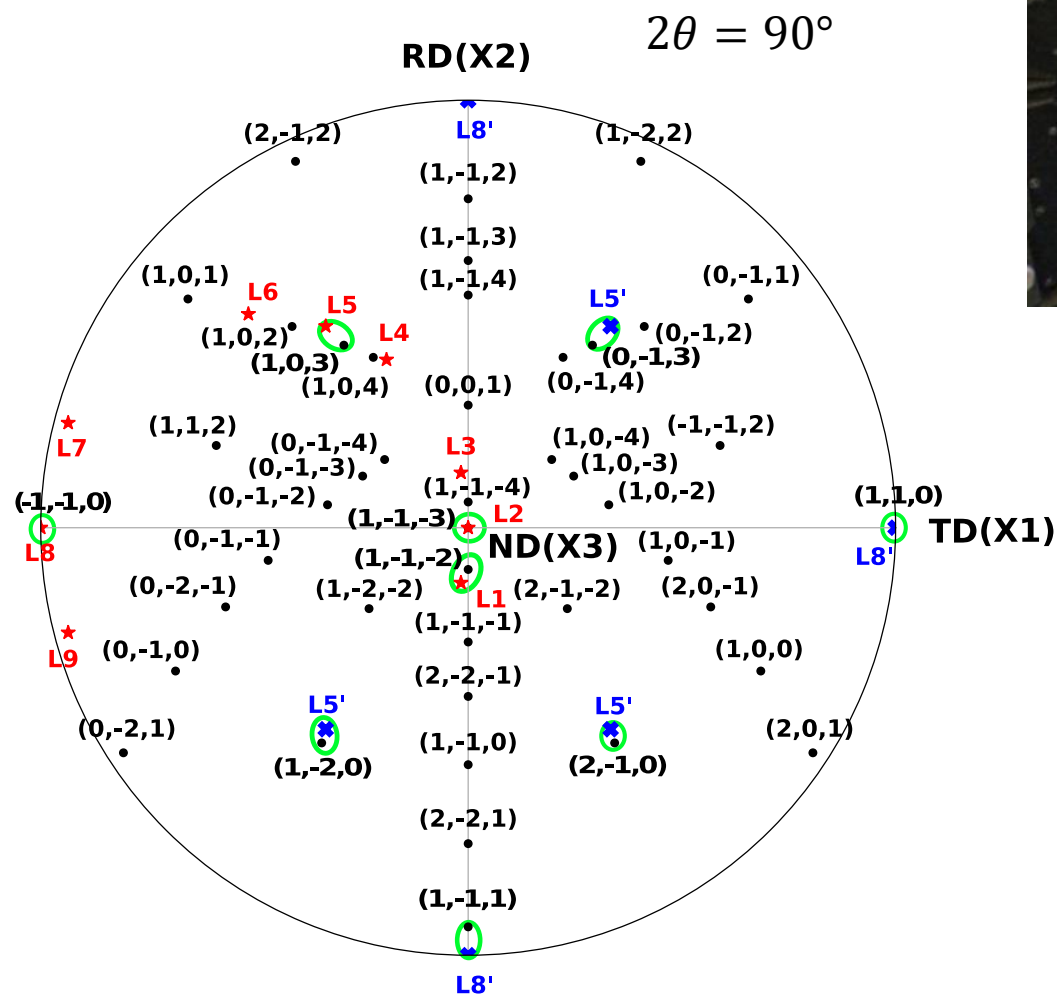
EPSILON - MDS diffractometer



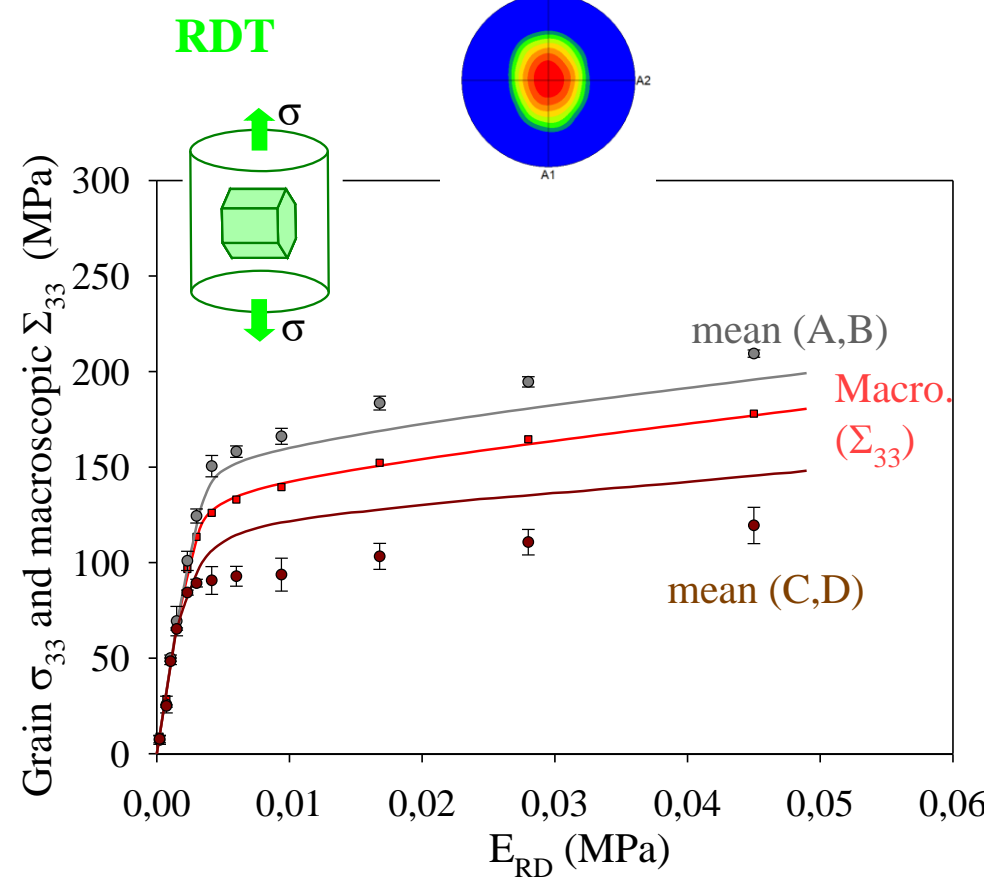
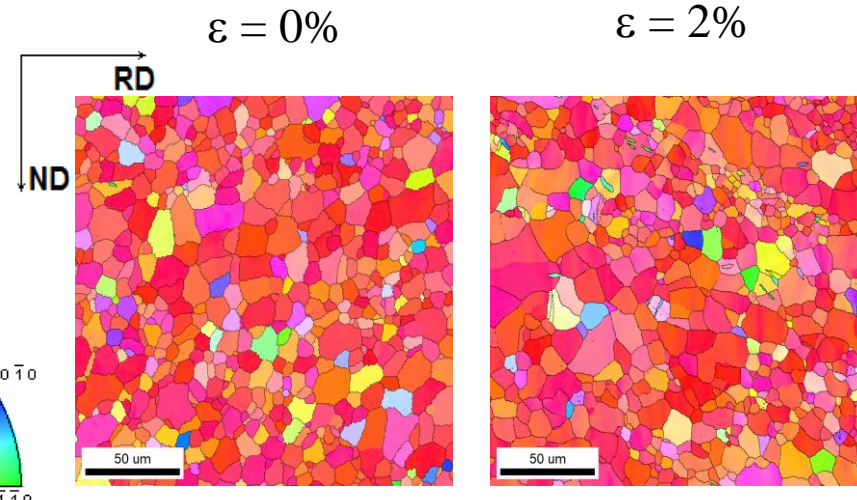
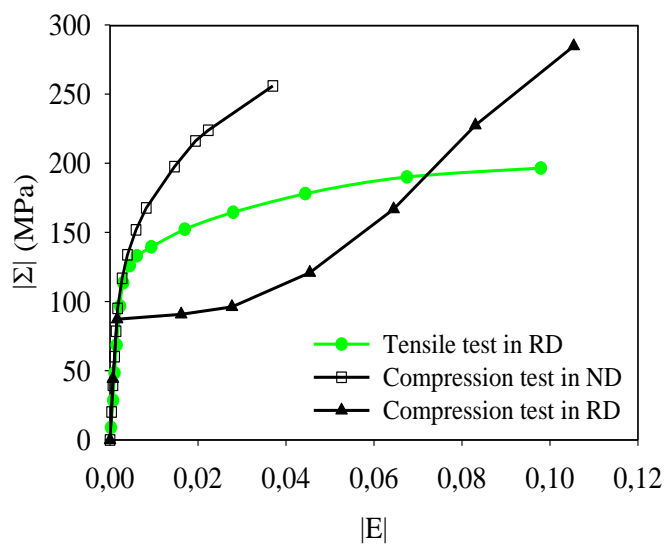
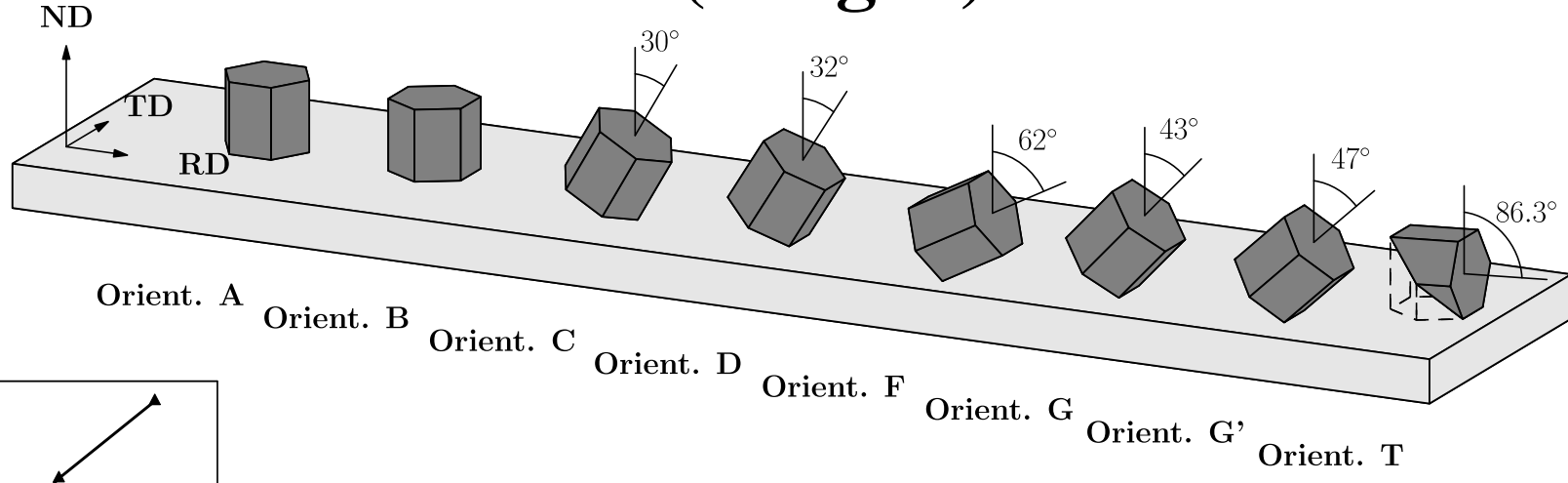
Orient. D

# TOF diffraction in JINR Dubna, Russia (NDC and RDC)

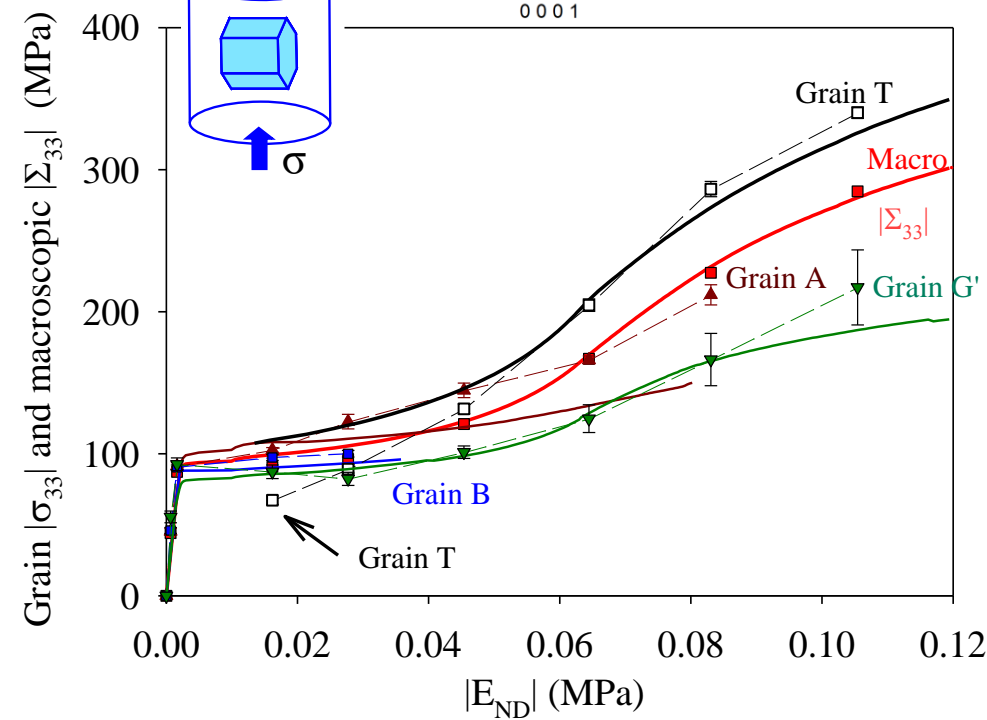
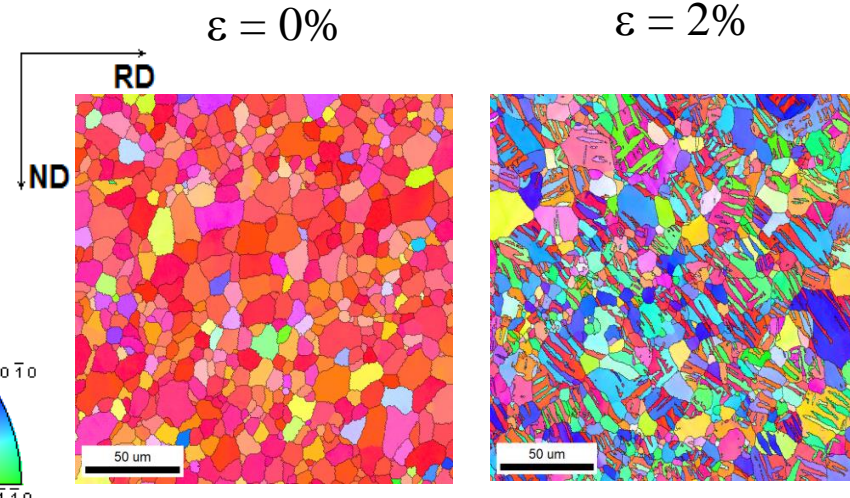
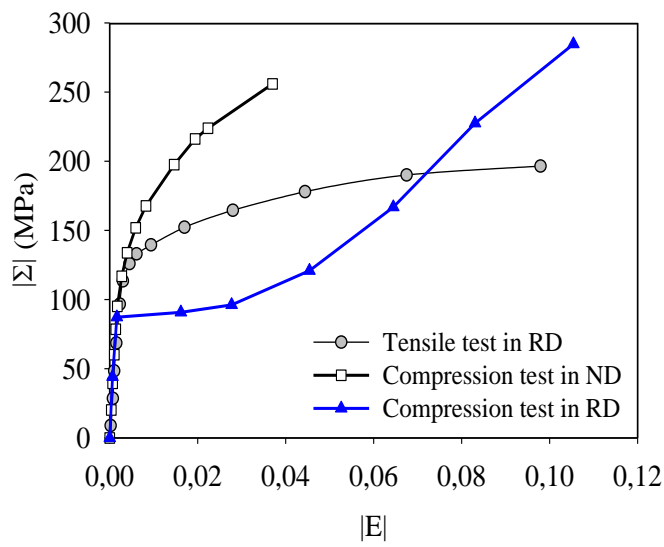
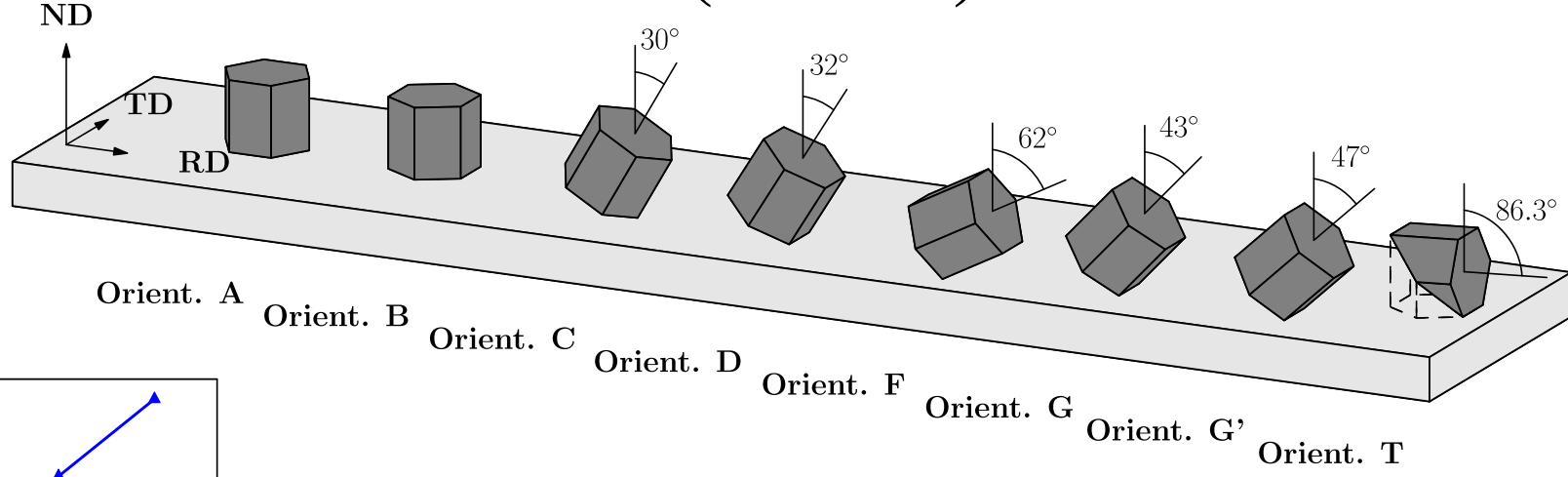
**Time of Flight:**  $d_{hkl} = \frac{hT}{2mL\sin \theta}$



# Stress localisation (Prague)

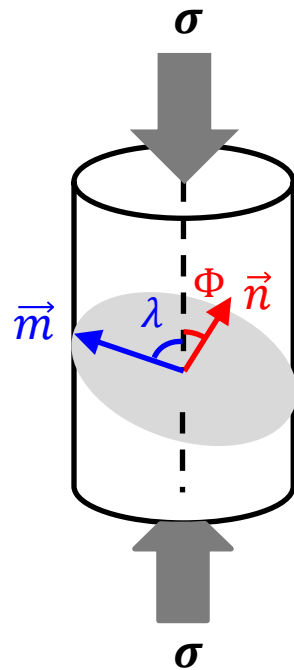


# Stress localisation (Dubna)



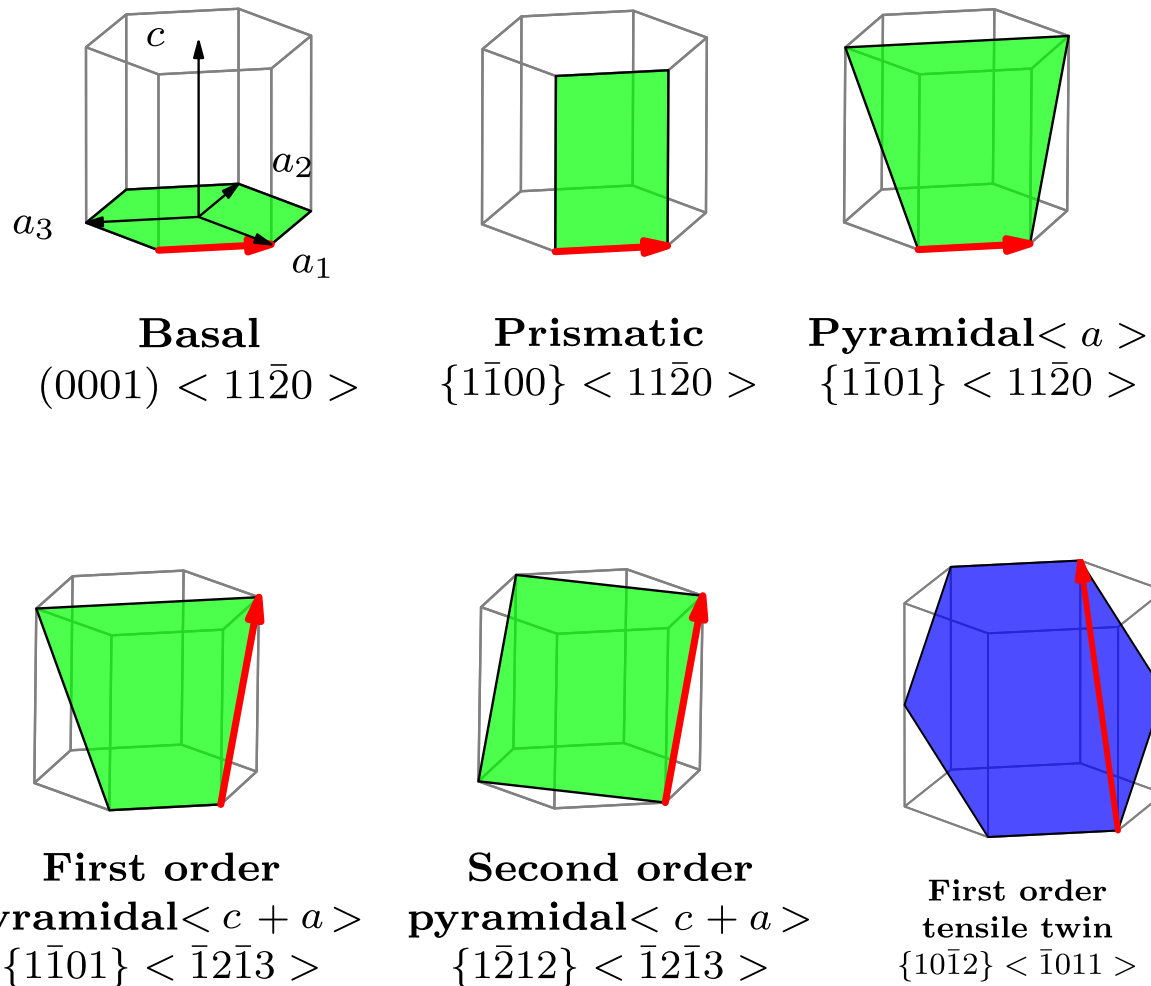
# Plastic deformation mechanisms in Mg alloy

# Resolved shear stress in Mg AZ31 alloy

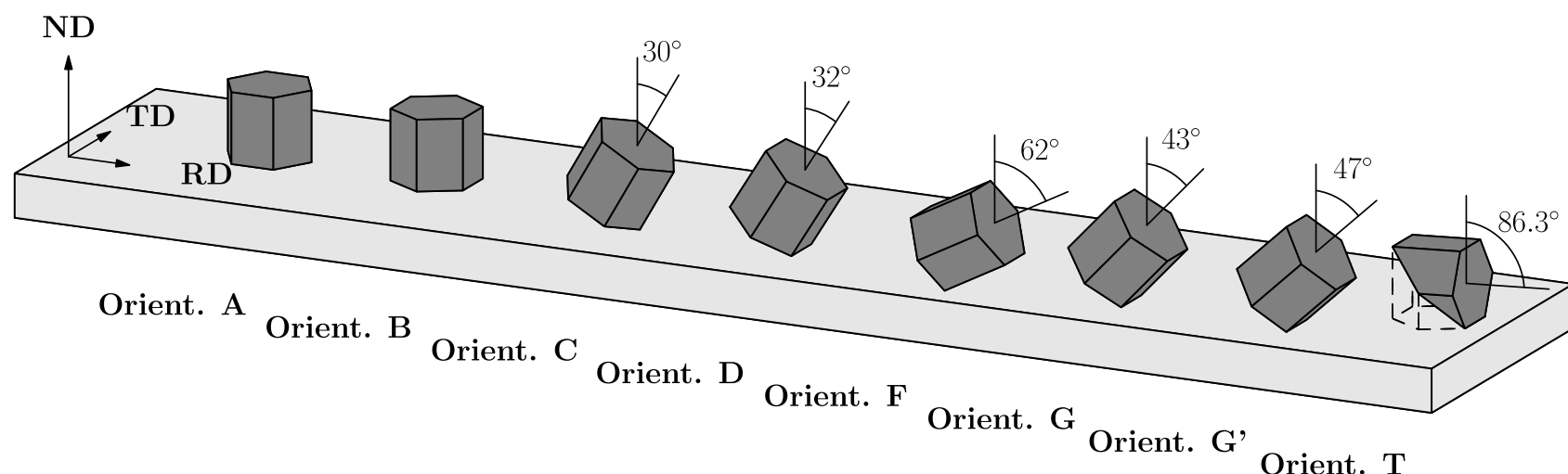
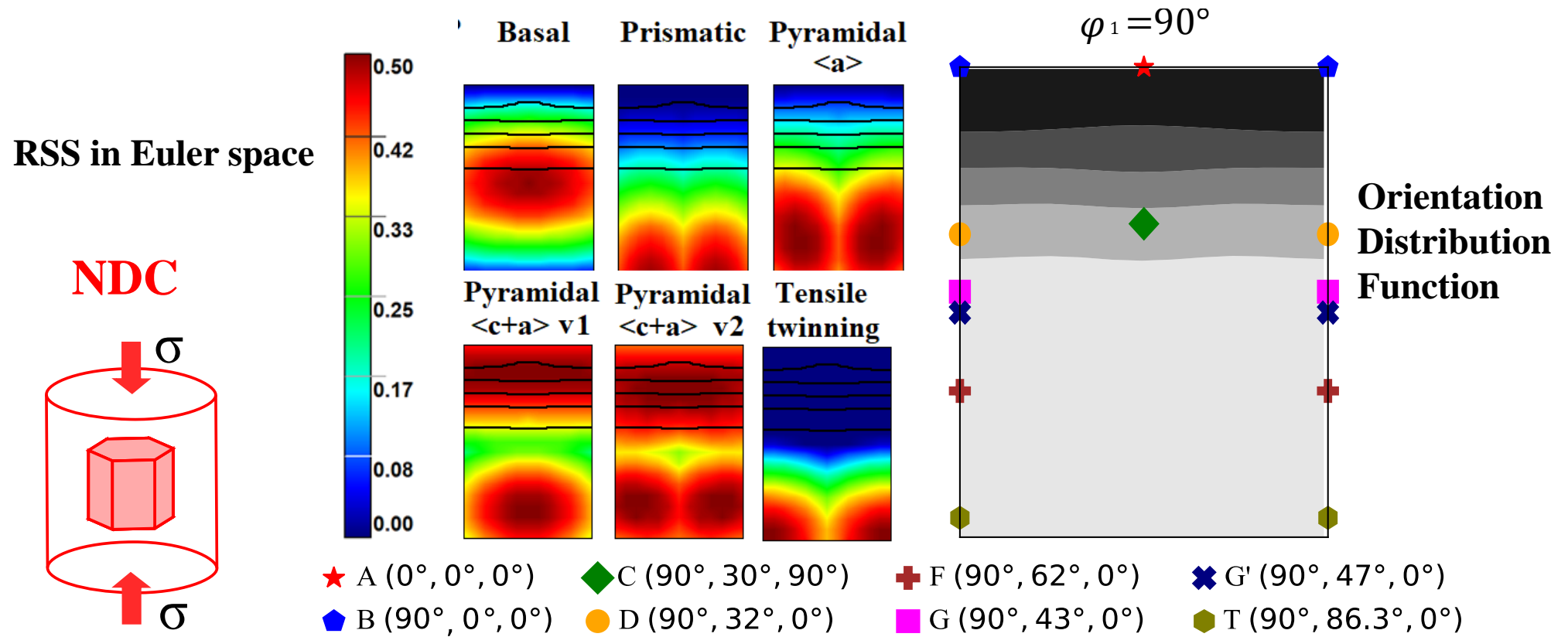


**Resolved shear  
stress (RSS):**

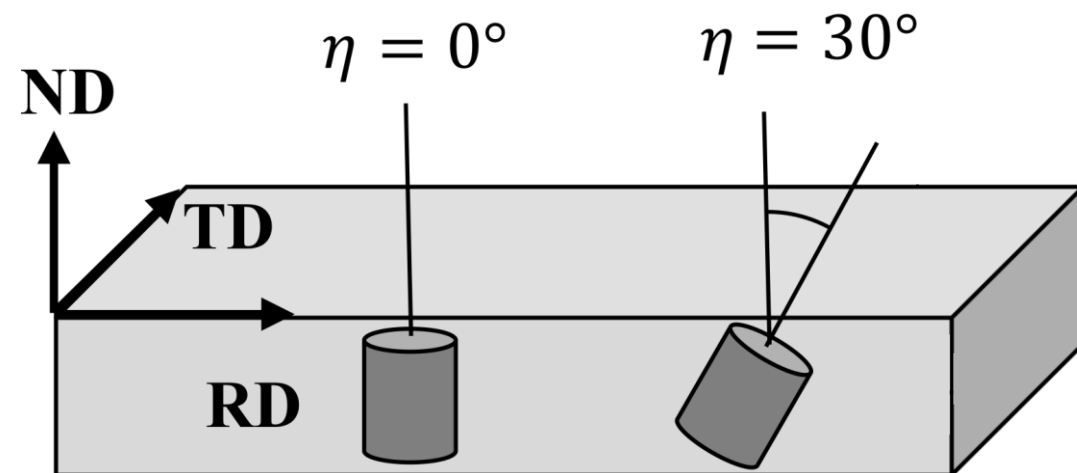
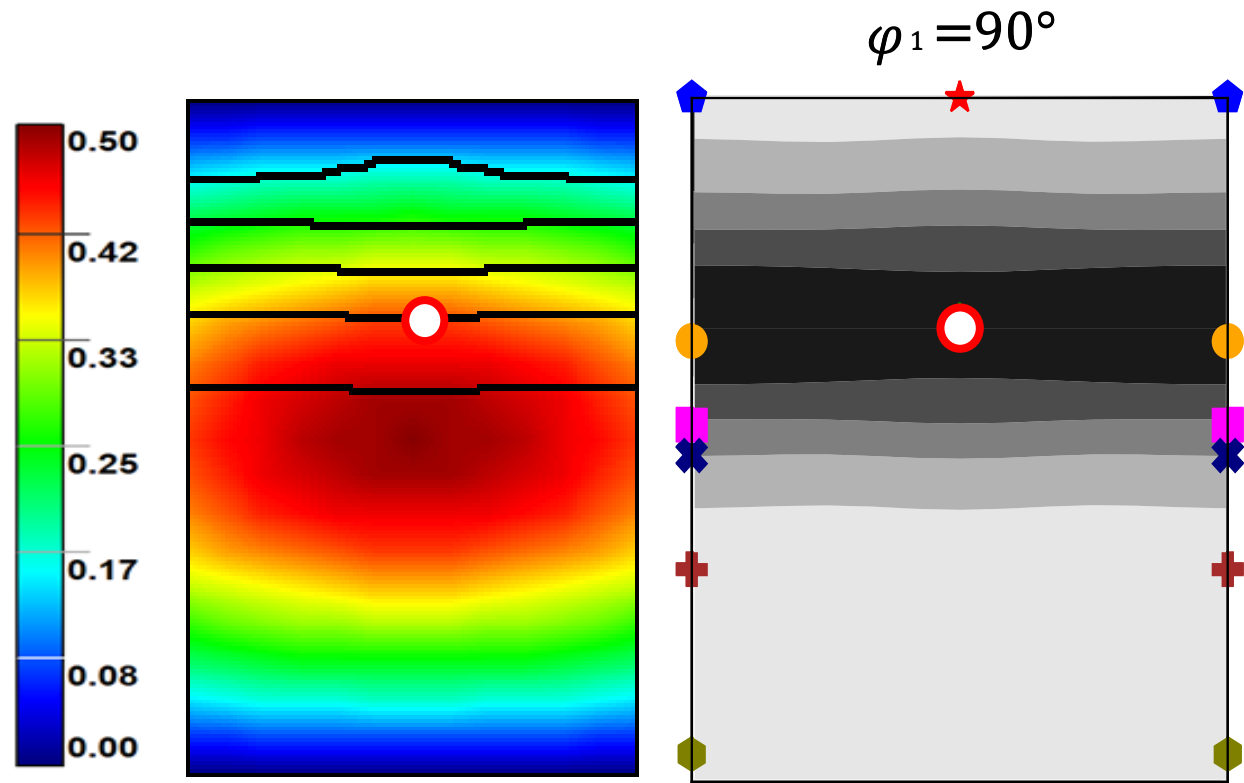
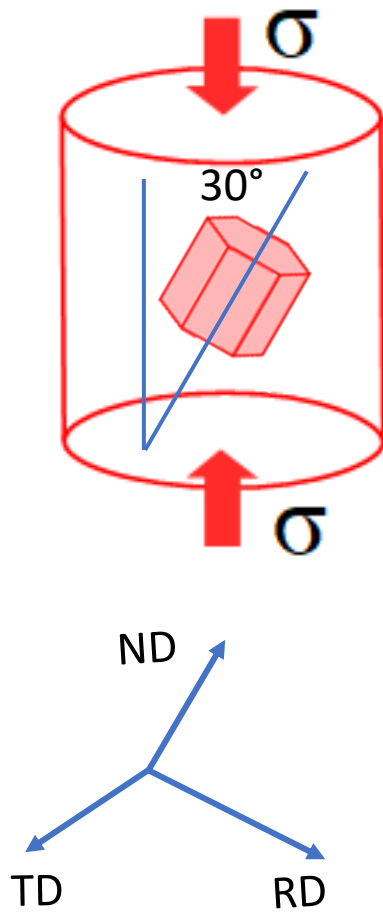
$$\tau = \vec{n} \cdot \vec{\sigma} \cdot \vec{m}$$



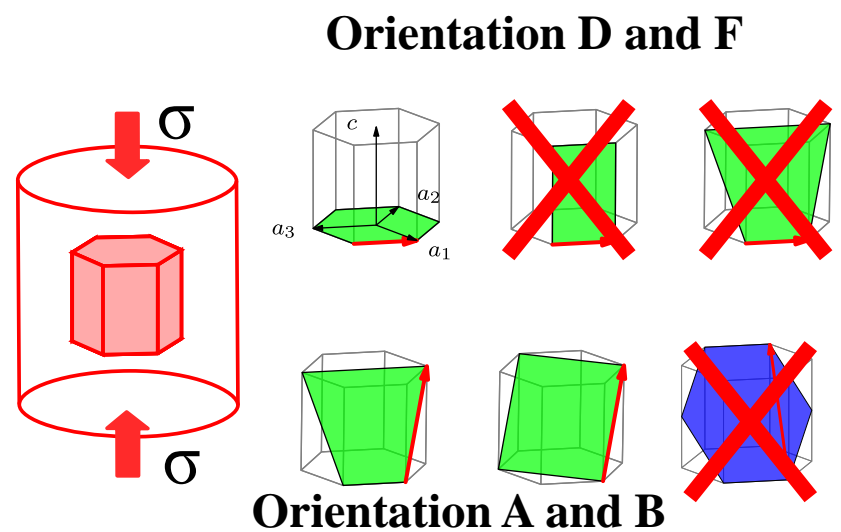
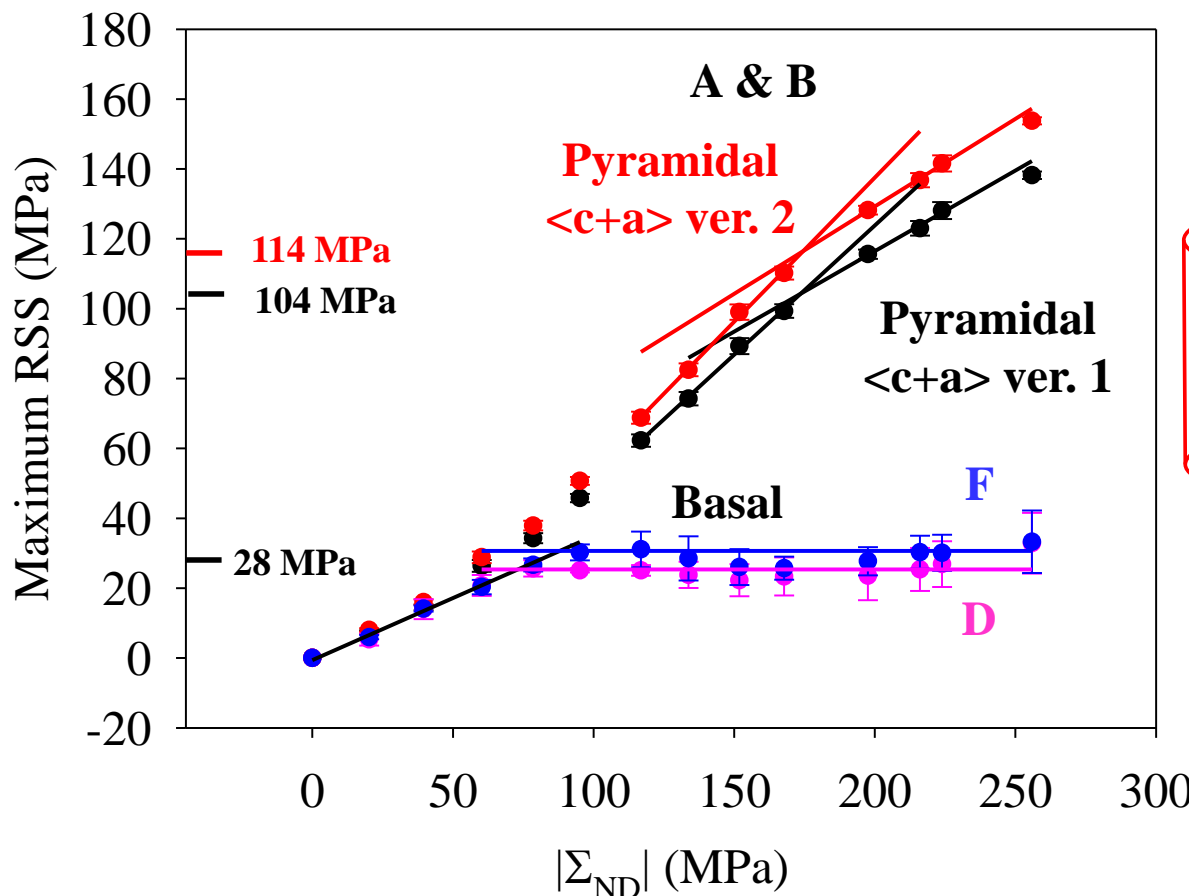
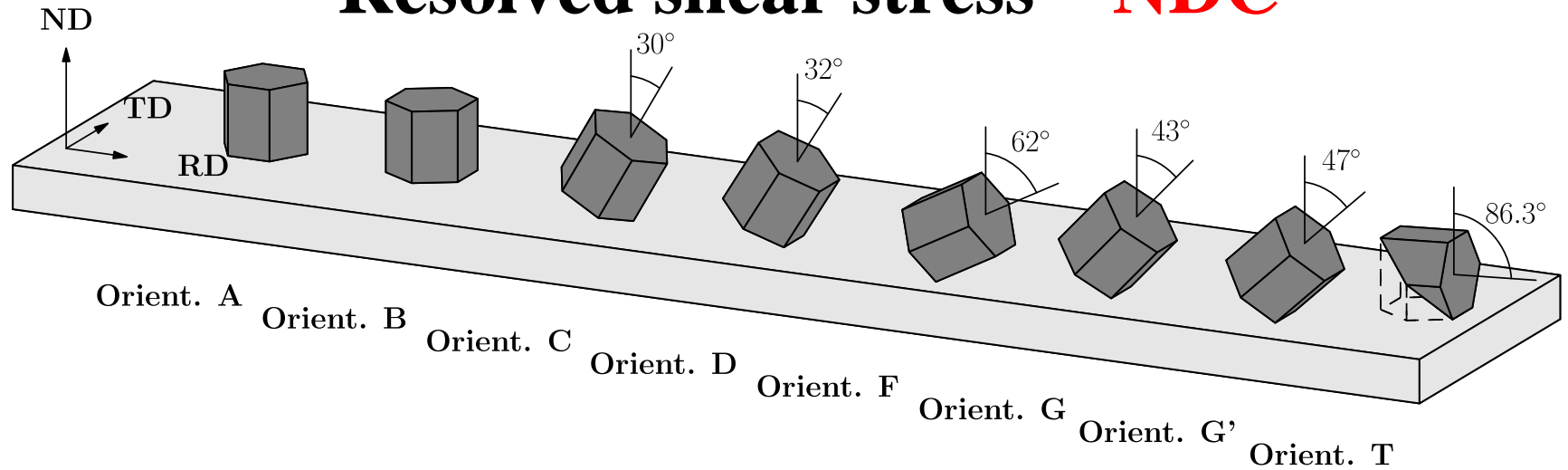
# Resolved shear stress in Mg AZ31 alloy



# Basal confirmation (Mg30)



# Resolved shear stress – NDC

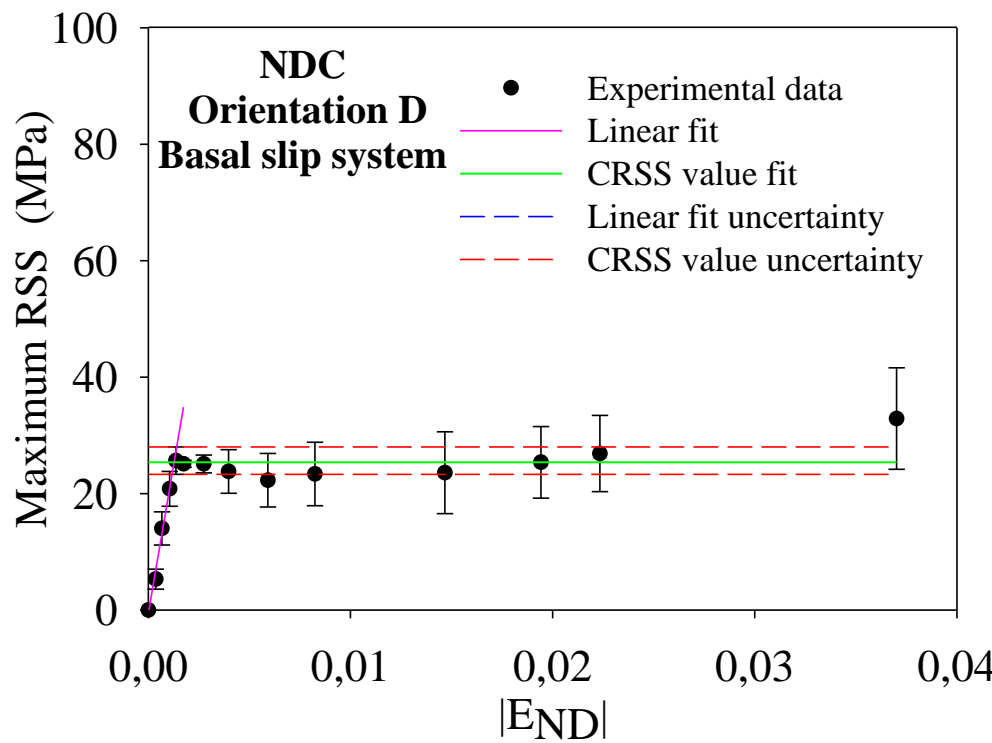


**CRSS:**

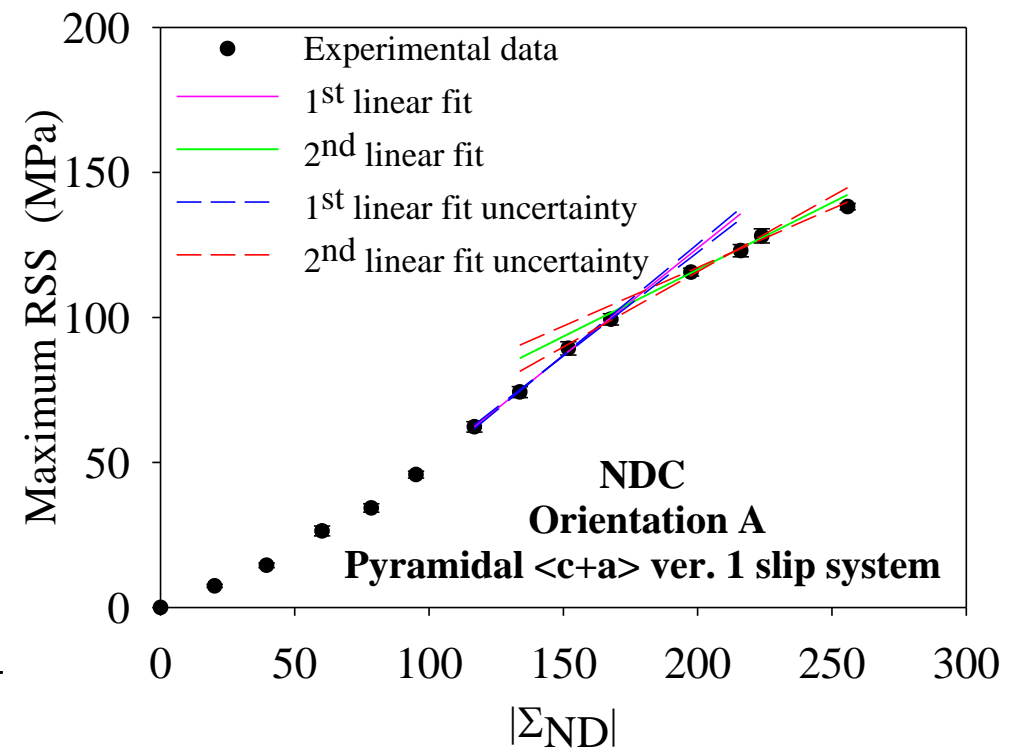
- Pyramidal  $\langle c+a \rangle$  v1 104 MPa
- Pyramidal  $\langle c+a \rangle$  v2 114 MPa
- Basal 28 MPa

# CRSS uncertainty

**Linear + constant**



**Linear + linear**



**Uncertainty based on points uncertainty**

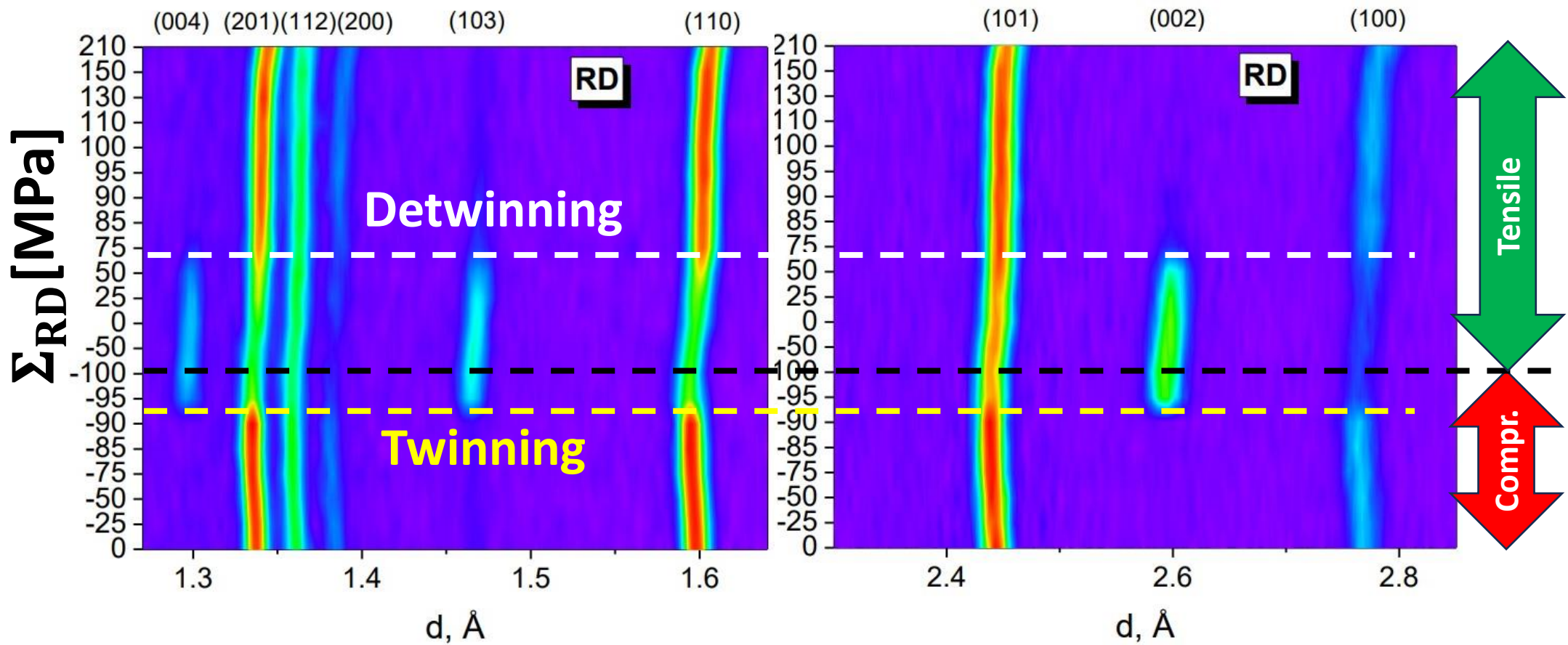
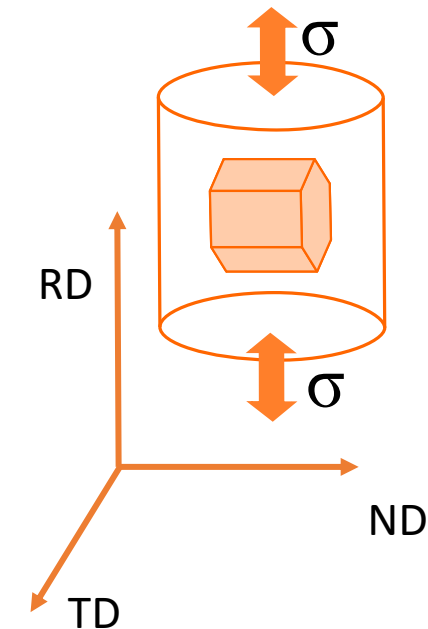
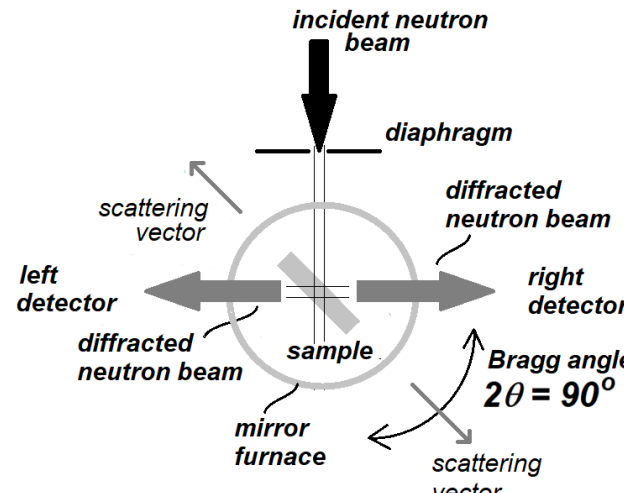
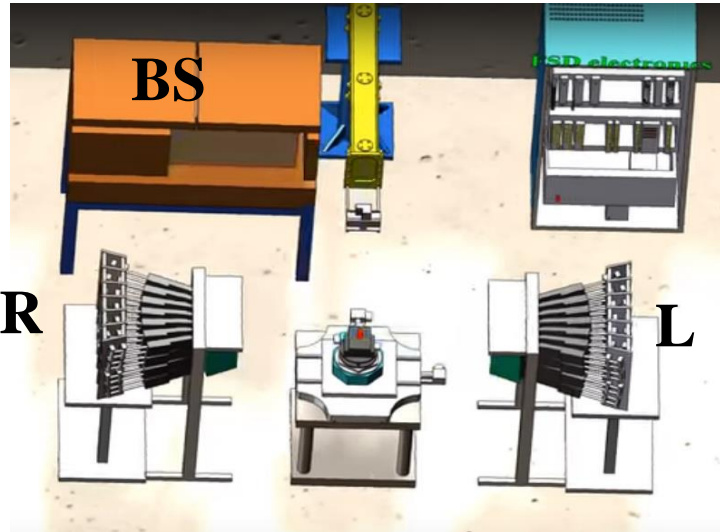
**Uncertainty based on linear regression**

# CRSS from experiments comparison

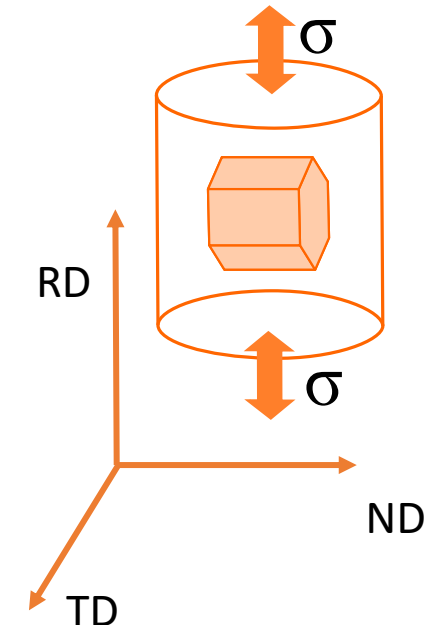
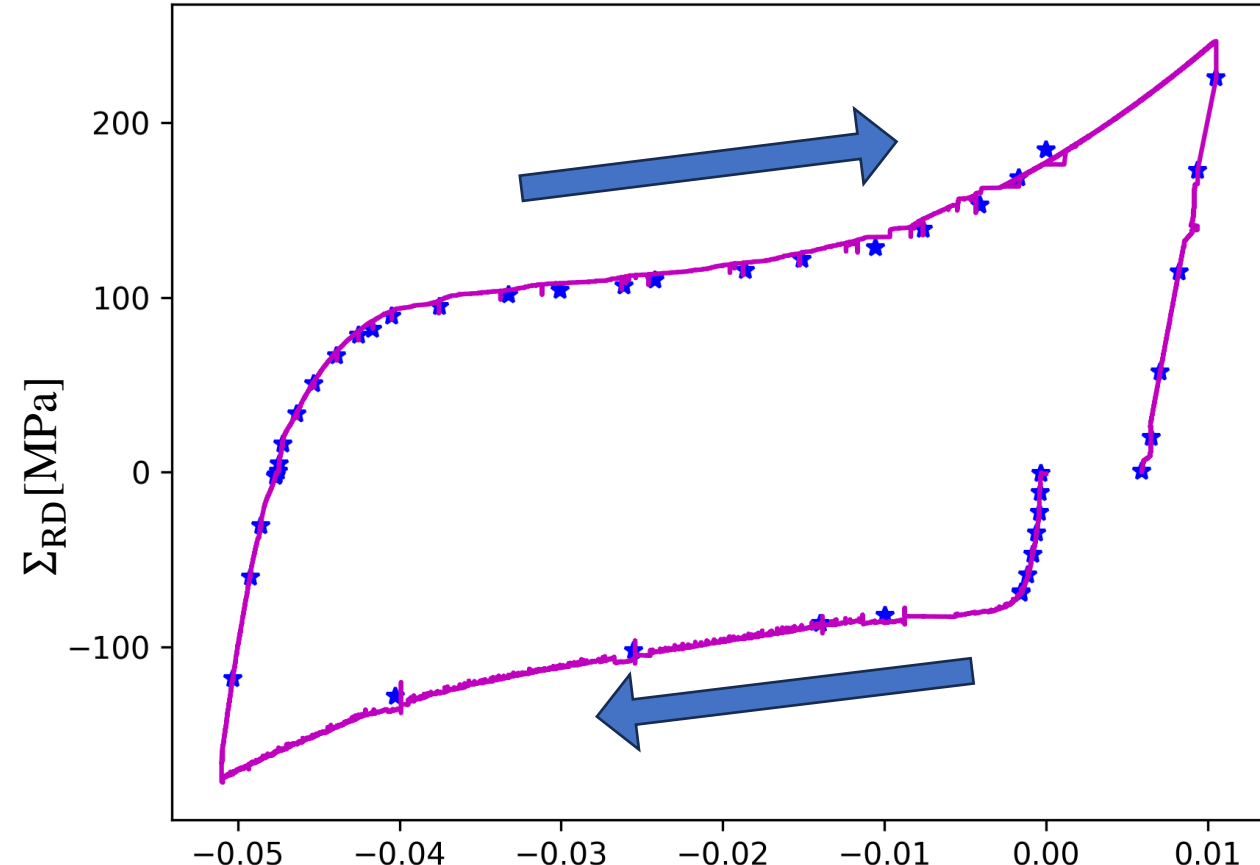
Slip systems	Miller-Bravais indices	$\tau_0$ (MPa)		
		Rez RDT	Dubna NDC, RDC	Rez NDC, RDC, Mg30
Basal $\langle a \rangle$	$\{0001\}\langle 11\bar{2}0 \rangle$	35	28.0 (3.1)	24.0(3.0)
Prismatic $\langle a \rangle$	$\{1\bar{1}00\}\langle 11\bar{2}0 \rangle$	>62	67.7 (7.9)	-----
Pyramidal $\langle a \rangle$	$\{1\bar{1}01\}\langle 11\bar{2}0 \rangle$	>62	59.7 (6.9)	-----
Pyramidal $\langle c+a \rangle$ v1	$\{\bar{1}011\}\langle 11\bar{2}3 \rangle$		104.4 (5.6)	117(10)
Pyramidal $\langle c+a \rangle$ v1 (in twin)			130 (108 – 145)	120.5(8.2)
Pyramidal $\langle c+a \rangle$ v2	$\{11\bar{2}\bar{2}\}\langle 11\bar{2}3 \rangle$		116.6 (3.5)	130(12)
Pyramidal $\langle c+a \rangle$ v2 (In twin)			144 (120 – 161)	134.3(9.1)
Twinning	$\{10\bar{1}2\}\langle \bar{1}011 \rangle$		49.1 (2.5)	45.5(1.6)

# Cycling load twinning and detwinning

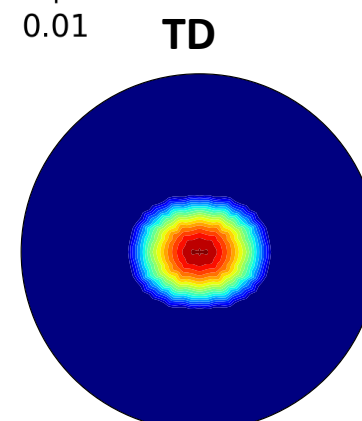
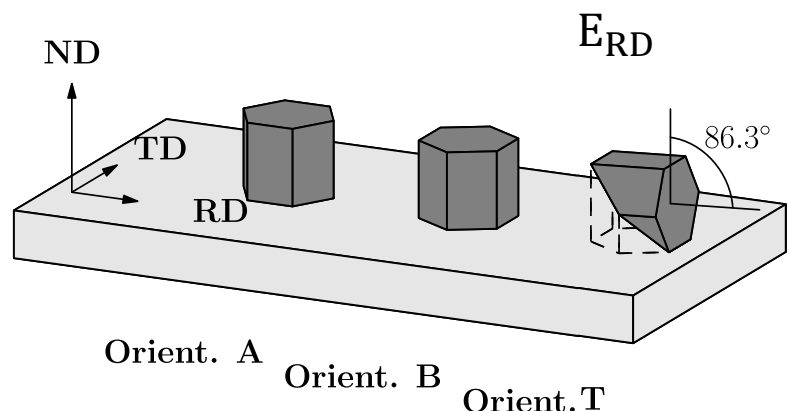
# Cycling load at FSD, Dubna



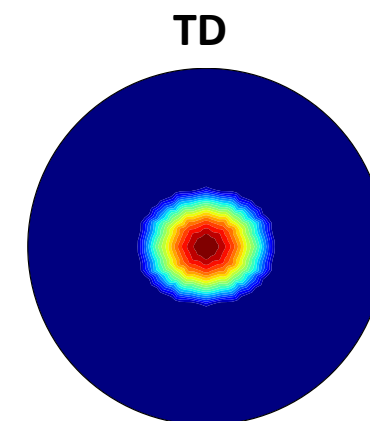
# Cycling load at HK9, NPI, Řež/Prague



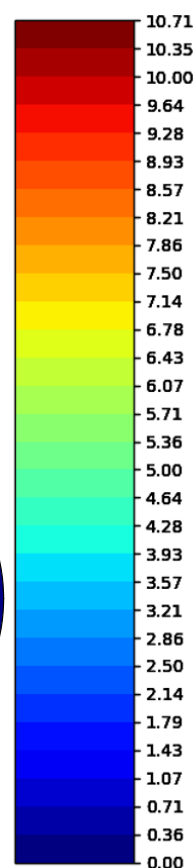
00.2 texture



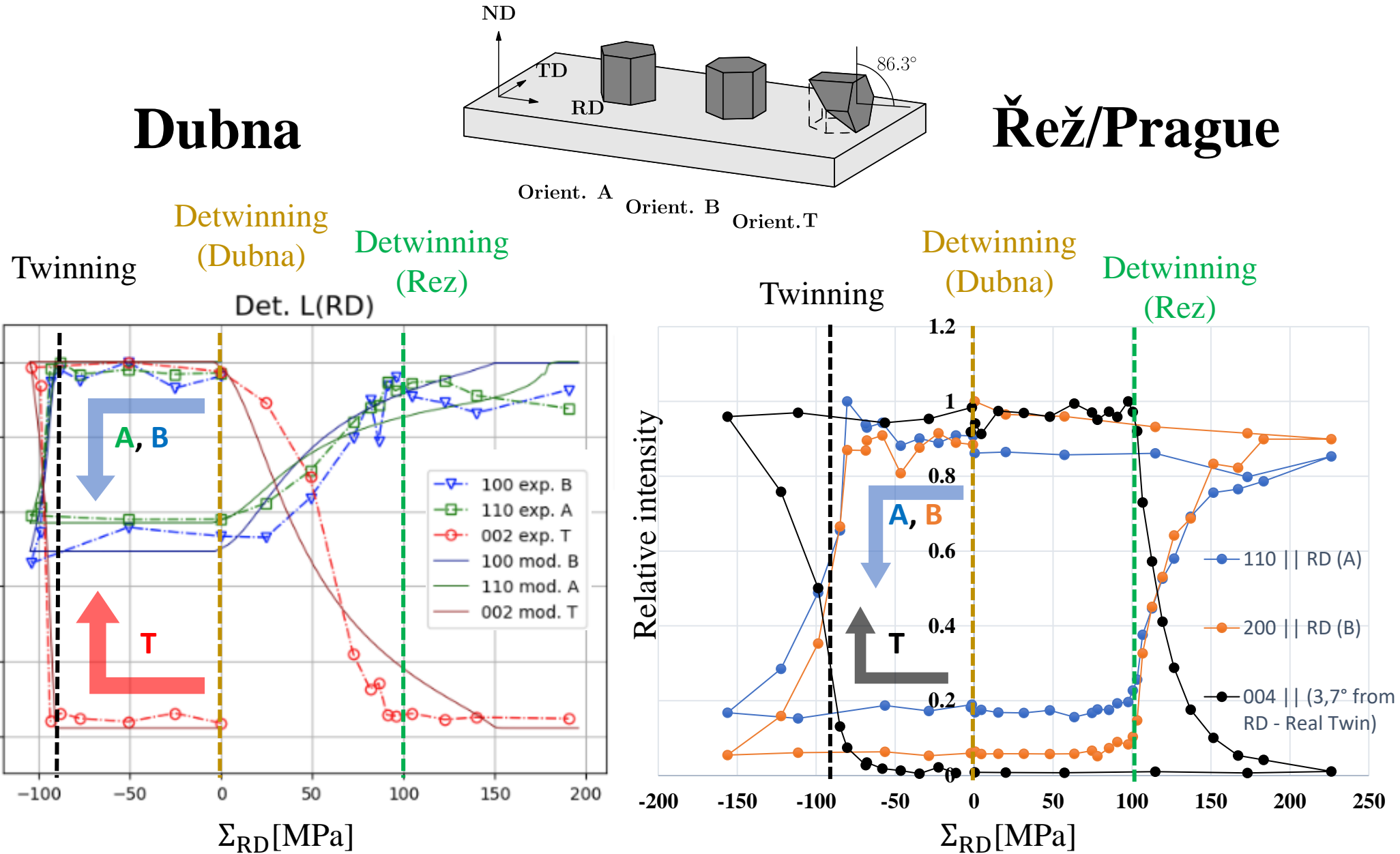
initial



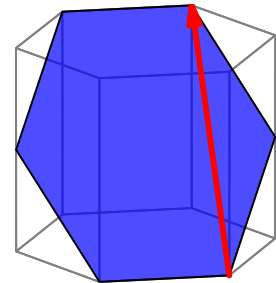
deformed



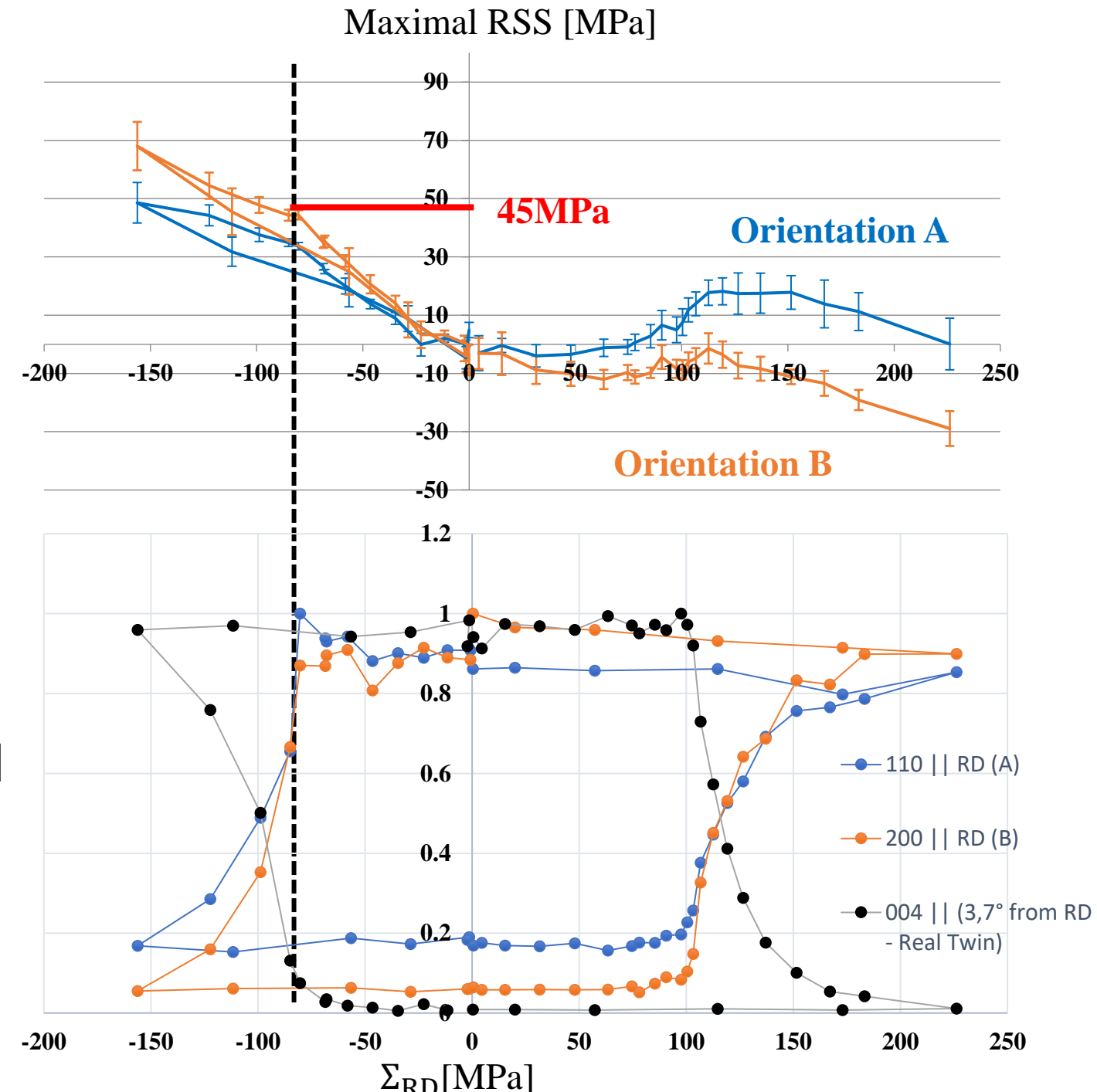
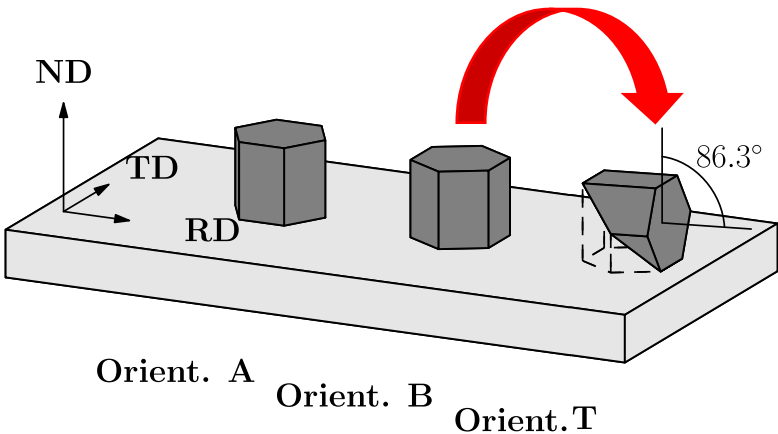
# Twinning and detwinning during cycle loading



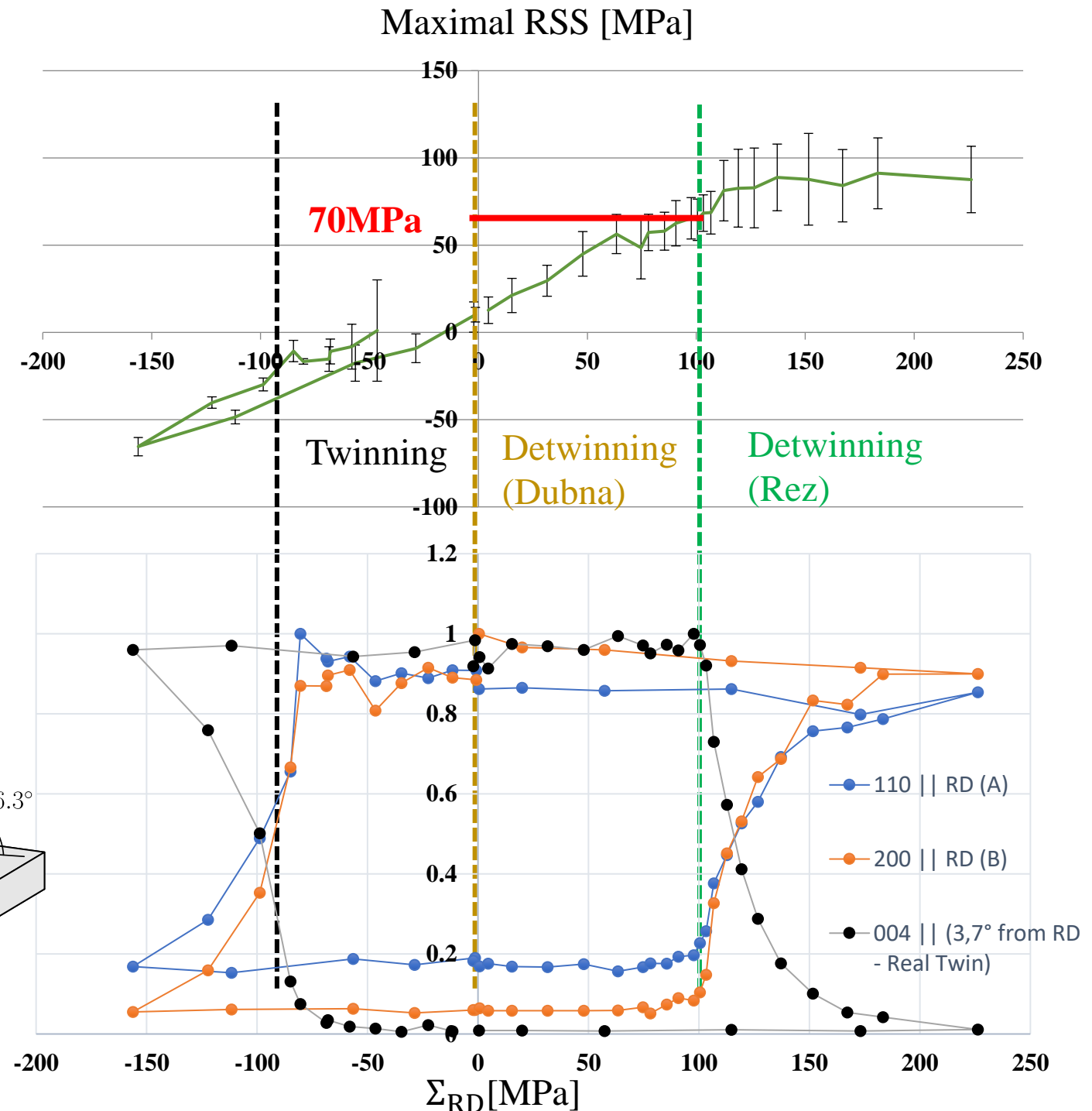
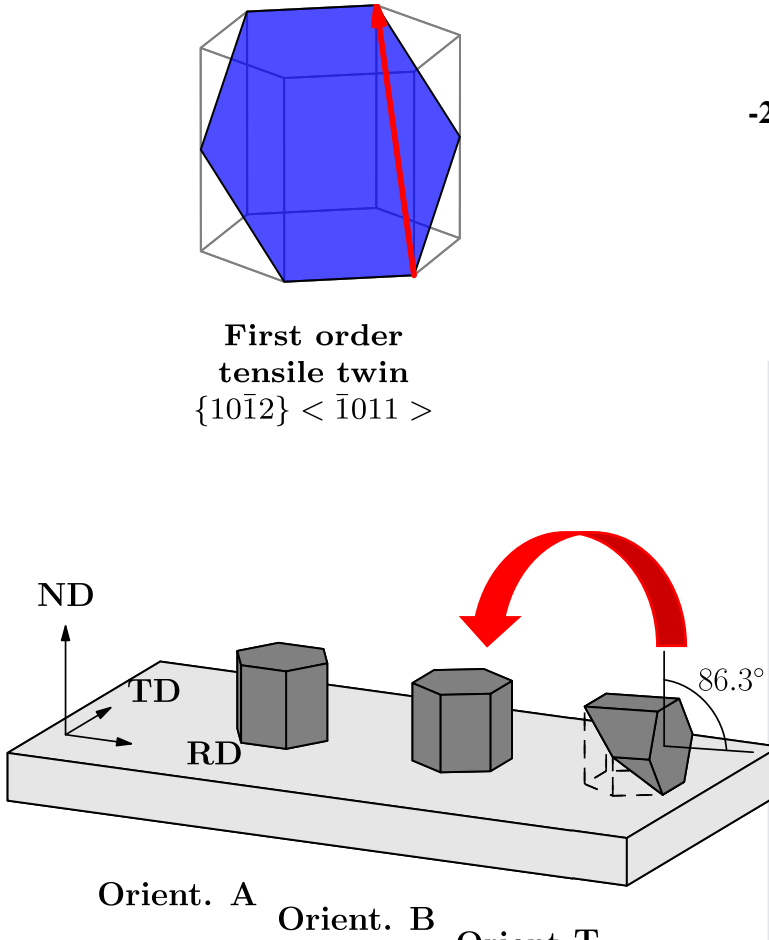
# Twinning during compression phase



First order  
tensile twin  
 $\{10\bar{1}2\} < \bar{1}011 >$



# Detwinning during tensile phase



# **Conclusions**

- 1. Diffraction methods for deformation study was developed**
- 2. For textured Mg AZ31 alloy stresses on different crystallite groups were determined directly from experiment**
- 3. Elastic-plastic deformation was described at grain scale in textured magnesium**
- 4. The CRSS values are unabiguously determined directly from experiment with uncertainties (model assumptions not used)**
- 5. For the first time detwinning CRSS value was measured using neutron diffraction**

# Acknowledgements

**This work was partially financed by grant from the National Science Centre, Poland (NCN) No. UMO-2017/25/B/ST8/00134 and UMO-2021/41/N/ST5/00394 .**

**P. Kot were personally supported in part by the European Union Horizon 2020 research and innovation program under Grant Agreement No. 857470 and from the European Regional Development Fund via Foundation for Polish Science International Research Agenda PLUS program Grant No. MAB PLUS/2018/8.**

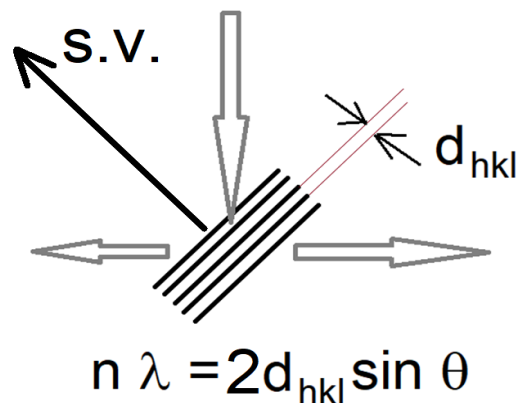
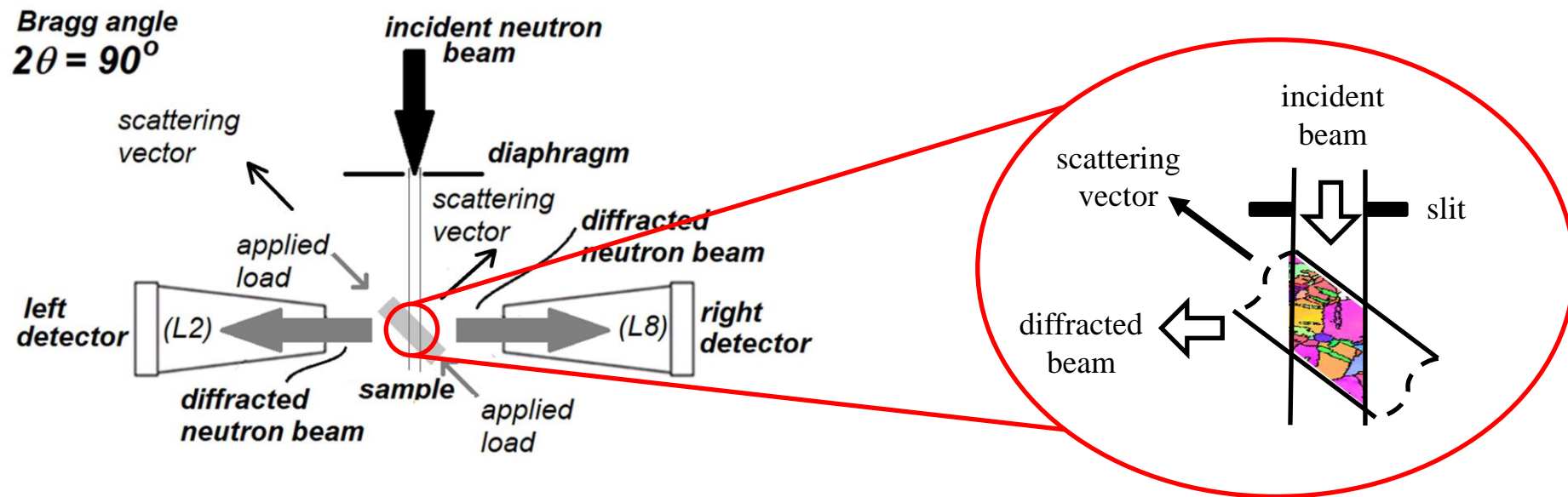
**The neutron diffraction experiments used in this work were performed during the period 2017-2019 at JINR in Dubna (Russia) and the purchase of samples/reagents/ancillary equipment was partly financed by the joint JINR/AGH projects nr PWB/254\_24/2018 and PWB/129-23/2019.**

**Thank you for your attention!**

# Backup slides

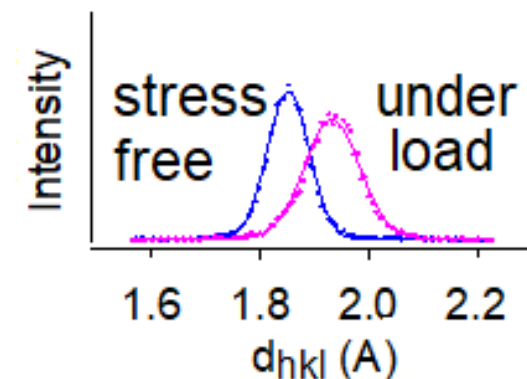
# Stress/strain measurement using diffraction

## In situ diffraction measurement under applied loads

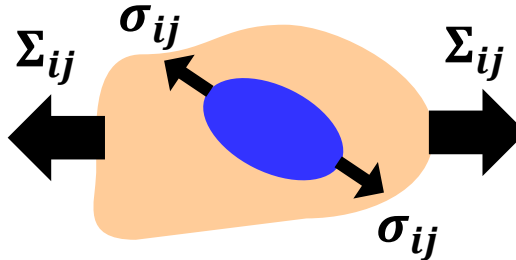


Relative lattice strain for loads:

$$\varepsilon_{hkl} = \frac{d_{hkl} - d_{hkl}^{initial}}{d_{hkl}^{initial}}$$

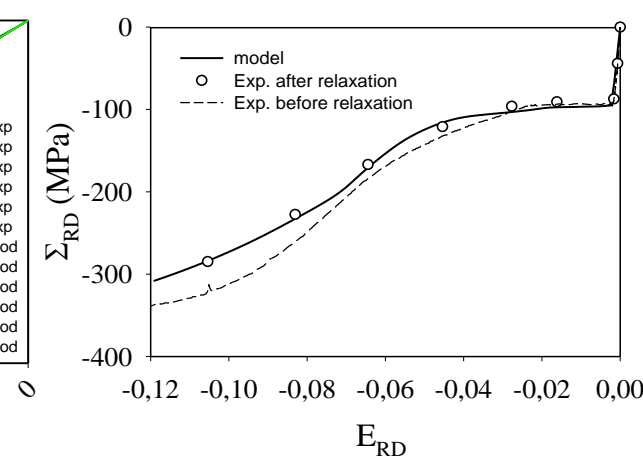
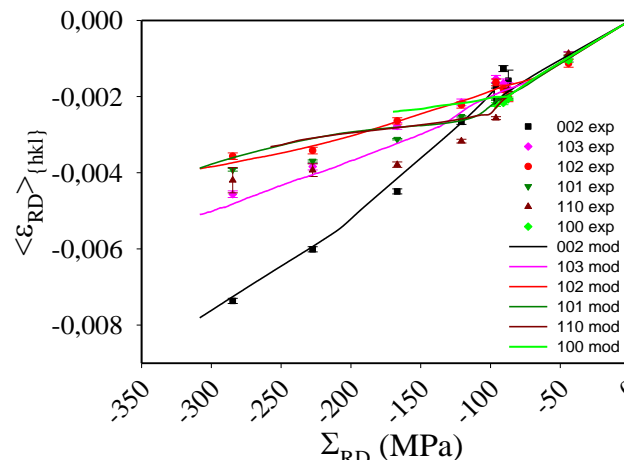
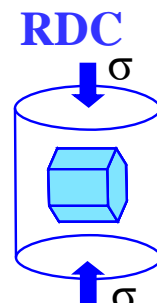
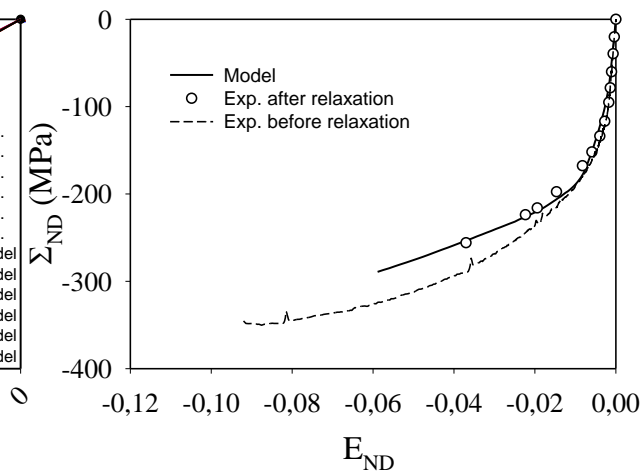
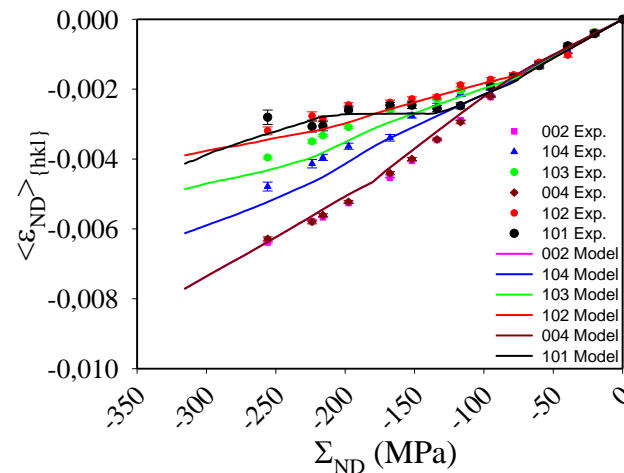
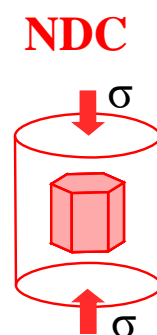
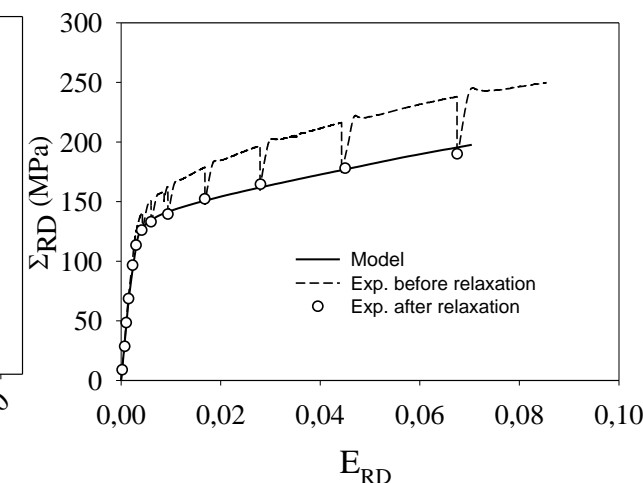
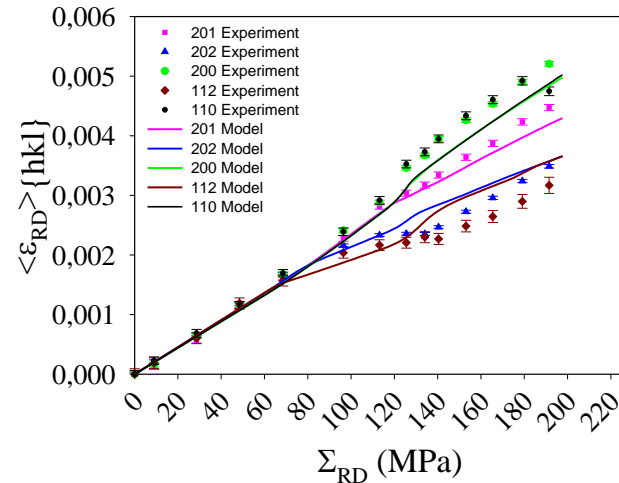
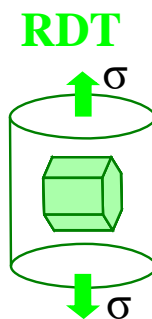


# EPSC model with experimental parameters

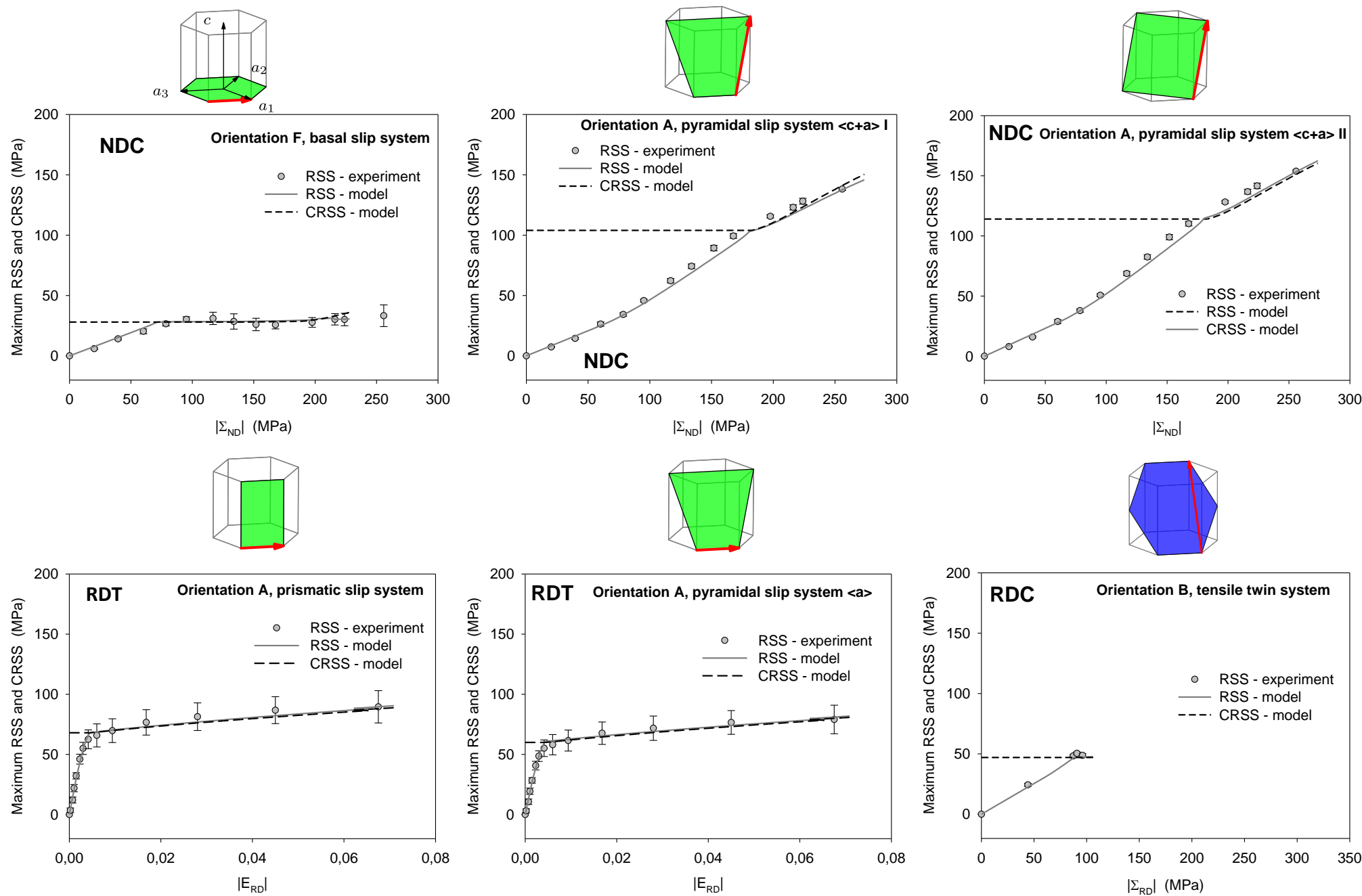


The values CRSS were directly determined from experiment and applied to verify model.

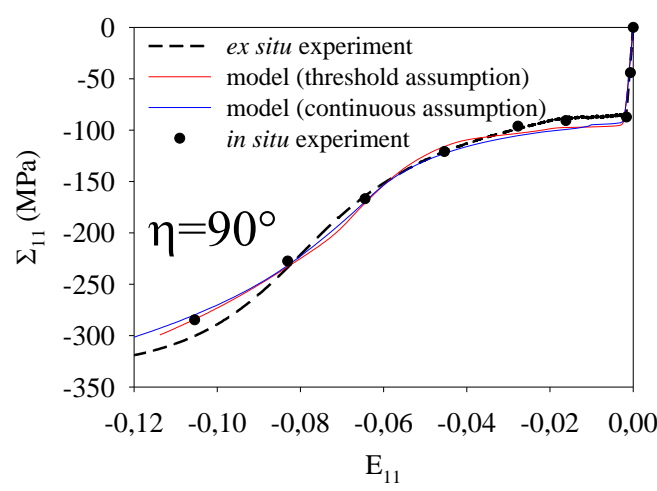
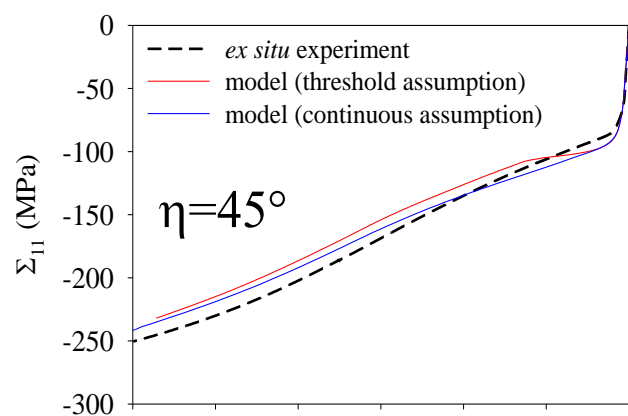
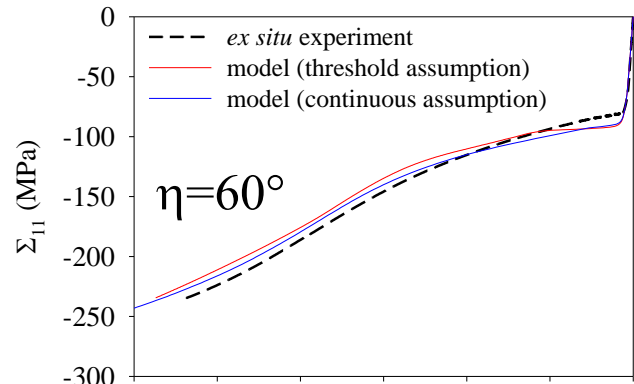
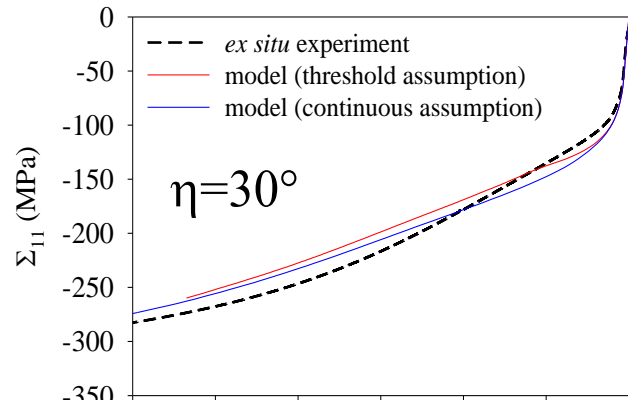
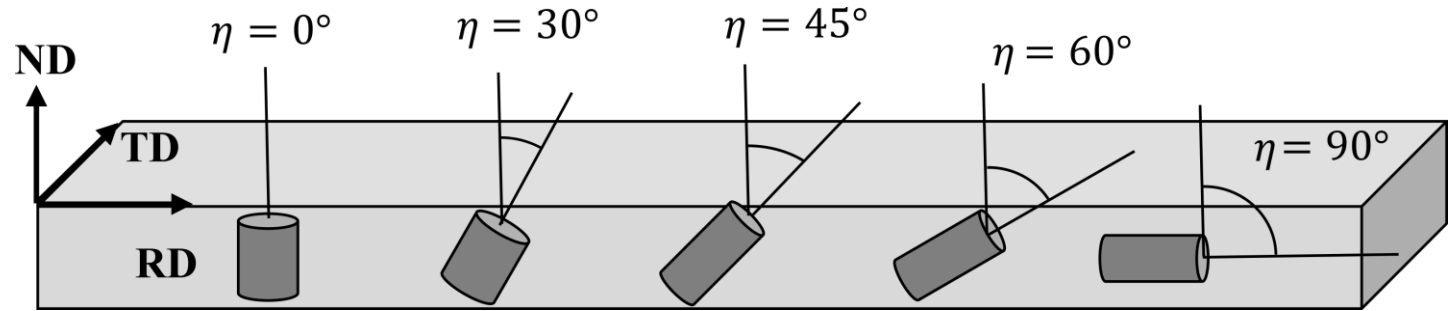
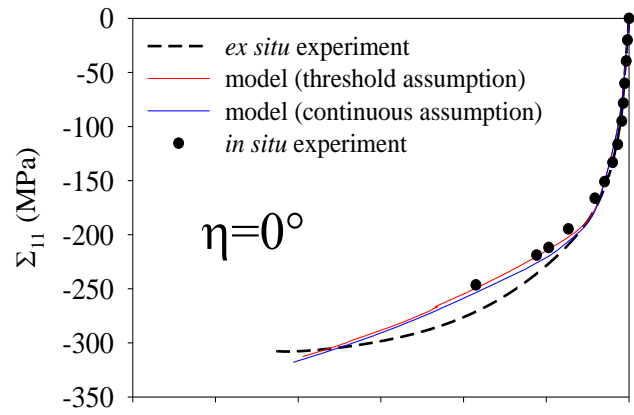
The Voce-law was used to determine hardening parameters.



# Maximum RSS and CRSS - model confirmation

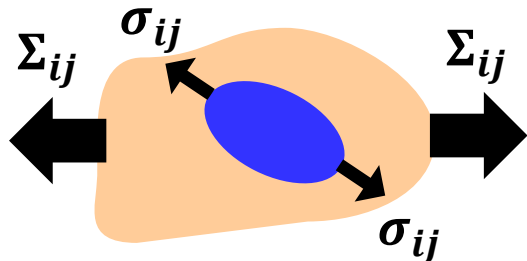


# Model vs ex-situ compression



Ex-situ compression tests were carried out for samples cut at different angles between ND and cylinder axis. The results were compared with model prediction. Two model assumptions were verified – continuous and threshold.

# Previous model results...



EPSC model with the Voce-law fitted to experimental data obtained in 2 directions.

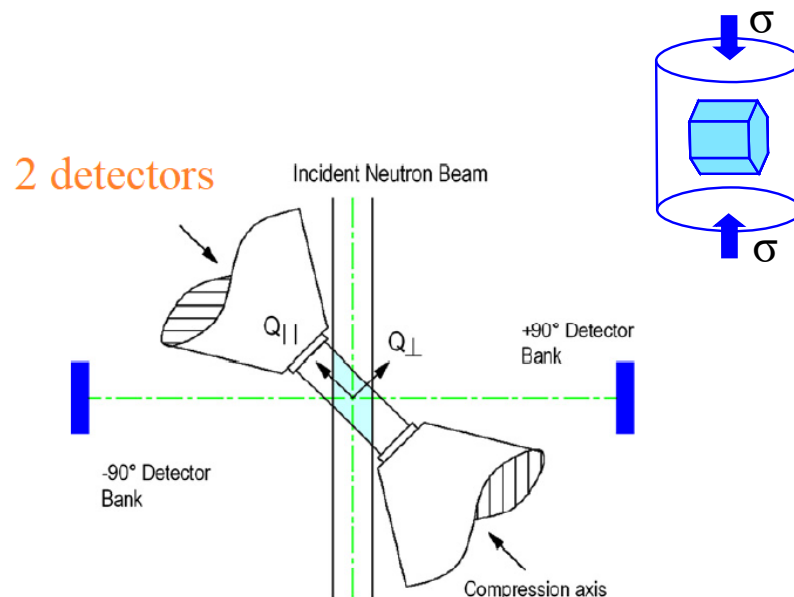
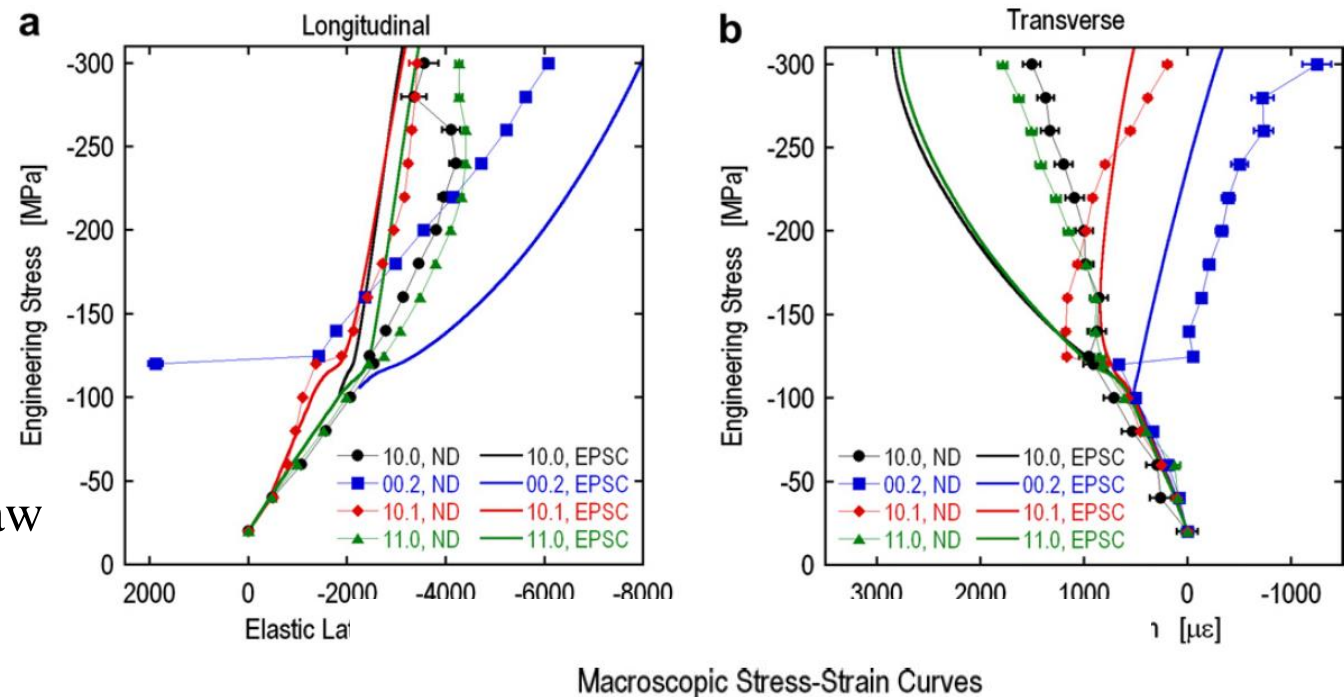


Fig. 3. Schematic of the in situ compression set-up of the SMARTS instrument.

Table 1  
CRSS and hardening parameters used for the two assumptions

Assumption	Initial twin fraction	Deformation system	$\tau_0$ (MPa)	$\tau_1$ (MPa)	$\theta_0$ (MPa)	$\theta_1$ (MPa)
Continuity	N/A	Basal	12	20	40	0
		Prism	60	20	40	0
		Pyramidal	100	117	2500	0
		Tensile twin	54	0	0	0
Fixed initial fraction	3%	Basal	12	20	240	0
		Prism	60	20	240	0
		Pyramidal	100	117	2000	0
		Tensile twin	60	0	0	0

# Comparison with literature

## Model + diffraction

H. Wang et al./International Journal of Solids and Structures 47 (2010) 2905–2917

**Table 1**

List of material constants for various self-consistent models.

Model	Mode	$\tau_0$
Affine	Basal	9
	Prismatic	79
	Pyramidal	100
	Tensile twin	47
Secant	Basal	13
	Prismatic	73
	Pyramidal	110
	Tensile twin	31
$m^{eff}$ ( $m^{eff} = 0.1$ )	Basal	17
	Prismatic	77
	Pyramidal	148
	Tensile twin	33
Tangent	Basal	21
	Prismatic	90
	Pyramidal	145
	Tensile twin	38

## Direct method

Slip system	CRSS from experiment $\tau_0$ (MPa)
Basal	28.0 (3.1)
Prismatic $\langle a \rangle$	67.7 (7.9)
Pyramidal $\langle a \rangle$	59.7 (6.9)
Pyramidal $\langle a+c \rangle$ ver. 1	104.4 (5.6)
Pyramidal $\langle a+c \rangle$ ver. 2	116.6 (3.5)
First order tensile twin	49.1 (2.5)